This is a repository copy of *20 Gbps Mobile Indoor Visible Light Communication System Employing Beam Steering and Computer Generated Holograms*.

White Rose Research Online URL for this paper:
http://eprints.whiterose.ac.uk/91285/

Version: Accepted Version

20 Gbps Mobile Indoor Visible Light Communication System Employing Beam Steering and Computer Generated Holograms

Ahmed Taha Hussein[1], Mohammed T. Alresheedi[2] and Jaafar M. H. Elmirghani[1]

School of Electronic and Electrical Engineering, University of Leeds, LS2 9JT, United Kingdom[1]

Department of Electrical Engineering, King Saud University, Riyadh, Saudi Arabia[2]

Abstract— **Visible light communication (VLC) systems have typically operated at data rates below 10 Gbps and operation at this data rate was shown to be feasible by using laser diodes (LDs), imaging receivers and delay adaptation techniques (DAT imaging LDs-VLC). However, higher data rates, beyond 10 Gbps, are challenging due to the low signal to noise ratio (SNR) and inter symbol interference (ISI). In this paper, for the first time, to the best of our knowledge, we propose, design and evaluate a VLC system that employs beam steering (of part of the VLC beam) using adaptive finite vocabulary of holograms in conjunction with an imaging receiver and a delay adaptation technique to enhance SNR and to mitigate the impact of ISI at high data rates (20 Gbps). An algorithm was used to estimate the receiver location, so that part of the white light can be directed towards a desired target (receiver) using beam steering to improve SNR. Simulation results of our location estimation algorithm (LEA) indicated that the required time to estimate the position of the VLC receiver is typically within 224 ms in our system and environment. A finite vocabulary of stored holograms is introduced to reduce the computation time required by LEA to identify the best location to steer the beam to the receiver location. The beam steering approach improved the SNR of the fully adaptive VLC system by 15 dB at high data rates (20 Gbps) over the DAT imaging LDs-VLC system in the worst case scenario. In addition, we examined our new proposed system in a very harsh environment with mobility. The results showed that our proposed VLC system has strong robustness against shadowing, signal blockage and mobility.**

Index Terms— **beam steering, location estimation, finite vocabulary of holograms, delay adaptation, imaging receiver, ISI, laser diodes, SNR.**

I. INTRODUCTION

Visible light communication (VLC) systems have become promising candidates to complement conventional radio frequency (RF) systems due to the increasingly saturated RF band and the potential high data rates that can be achieved by VLC systems [1], [2]. Over the last decade, significant research effort has been directed towards the development of VLC systems due to their numerous advantages over RF systems, such as the availability of simple transmitters (light emitting diodes, LEDs) and receivers (silicon photo detectors), better security at the physical layer and hundreds of THz of license-free bandwidth. However, there are several challenges facing VLC systems to achieve high data rates (multi gigabits per second). These challenges include the low modulation bandwidth of the LEDs and inter symbol interference (ISI) due to multipath propagation.

Various techniques have been proposed to mitigate the limitations (low modulation bandwidth of LEDs and ISI) in VLC systems to achieve high data rates [3], [4], [5]. Ongoing research activities intend to increase the data rates of indoor VLC systems, for example by utilizing massive MIMO and OFDM techniques [6], [7]. Notable techniques include the use of discrete multi-tone (DMT) modulation, wavelength division multiplexing (WDM) and Red Green Blue (RGB) LEDs, which resulted in an aggregate throughput VLC data transmission of 3.4 Gbps [8].

However, these techniques added complexity to the transceiver in the VLC system.

A prototype from the Sandia lab proved that laser sources can provide a practical white light illumination source [9]. Recently, different types of laser diode (LD) light were investigated to generate white light, while a blue laser in combination with yellow emitting YAG:Ce resulted in a luminous flux of 252 lumens and luminous efficacy of 76 lm/W [10], [11]. Previous work has shown that significant enhancements in the VLC system data rates can be achieved by replacing LEDs with LDs coupled with the use of an imaging receiver instead of the conventional wide field of view (FOV) receiver [12], [13]. In addition, performance evaluations were carried out for a mobile multi-gigabit VLC system in two different environments [14]. A rate of 10 Gbps in a realistic environment has been shown to be possible with a VLC system when a delay adaptation technique in conjunction with laser diodes and imaging receiver were used with a simple modulation format (on off keying, OOK) and without the use of relatively complex wavelength division multiplexing approaches [12]. Significant improvements were shown to be possible when a VLC relay assisted system is combined with an imaging receiver and a delay adaptation technique [15]. However given typical parameters, the latter system cannot provide a throughput beyond 10 Gbps due to its low signal to noise ratio (SNR). The concept of using RGB LDs for indoor VLC systems has also been studied in [16]. It investigates the communication capabilities of off-the-shelf LDs in a number of scenarios with illumination constraints. It is expected to achieve 100 Gbps at standard illumination level when using WDM and parallel streams [16]. Recently, a 4 Gbps VLC system employing commercial RGB LDs has been demonstrated at room temperature [17].

Beam steering has been widely investigated in communication systems to maximise the SNR at the receiver [18], [19], [20]. Therefore, beam steering can also be an attractive option to consider in VLC systems to enhance the system performance. Recently, transmission beam steering for multi input multi output (MIMO) infrared optical wireless (IR-OW) systems with intensity modulation and direct detection has been developed [21]. In addition, recent work has demonstrated optical wireless energy transmission using optical beam steering and beam forming with a spatial light modulator (SLM). They focused light on the desired target using optical beam steering and beam forming to transfer optical wireless energy [22].

A VLC beam steering array can be constructed using electronically controlled mirrors in front of the receiver. An inexpensive approach that can be used to provide good link quality during mobility is to use mirrors with piezoelectric actuators in front of the receiver [2], [23]. Another approach is the tilting of the transmitter and receiver together using piezoelectric actuators that are controlled electronically. As with the mirror method, the tilting method also needs to be controlled

1

by an electronic circuit. However, these methods lead to a bulky receiver and cannot be used for mobile devices [2].

Recently, various approaches for VLC indoor positioning systems have been researched [24], [25]. VLC systems are a promising solution for indoor positioning due to many features. Firstly, there is better positioning accuracy (few millimetres) compared to radio wave systems, since VLC suffers less from interference and multipath effects. Secondly, VLC positioning systems can be used in environments where radio positioning systems are restricted, such as in hospitals [26].

Beam angle adaptation has been shown to be an effective technique that can help optimize the distribution of the diffusing spots in order to maximize the receiver's SNR, regardless of the transmitter's position, the receiver's orientation and the receiver's field of view (FOV). Simulation results have shown that a significant performance improvement can be achieved in a mobile IR-OW system that employs beam angle adaptation in a line strip multi-beam system (LSMS) [18], [19]. The improvements achieved are however at the cost of complex system design associated with LSMS. The complexity is associated with the computation time required to identify the optimum spot location, as well as the time needed to generate the hologram that generates beams at the optimum angles.

The work presented in this paper aims to address the impairments of VLC systems and provide practical solutions, hence achieving data rates beyond those reported in [12]-[15]. In this paper, for the first time to the best of our knowledge, we propose a novel location estimation algorithm (LEA) (based on beam angle adaptation) and beam steering (BSR) technique to improve the SNR of a VLC system at high data rates (20 Gbps and beyond). To reduce the system complexity, we introduce a new adaptive finite vocabulary hologram approach for beam steering making use of simulated annealing optimization. To best of our knowledge this represents the first time these techniques are used in VLC systems. The holograms are pre-calculated and stored in the proposed system (each is suited for a given (range of) transmitter and receiver locations) and eliminate the need to calculate holograms real time at each transmitter and receiver location. The concept of finite adaptive computer-generated holograms has been recently proposed in IR-OW [27], [28] and it is adapted here for the first time to VLC systems.

The first step is to estimate the receiver location using the LEA algorithm then the BSR technique steers part of RGB-LDs white light to the VLC receiver, which leads to enhanced received SNR. The enhancement in the signal strength by the BSR approach can improve the transmission distance. Imaging receivers were shown to be attractive and efficient in mitigating the effects of ambient light and pulse spread in infrared optical wireless systems [29], [30], [31], [32]. In our previous work we proposed the use of an imaging receiver for a VLC system to provide a robust link and mitigate multipath dispersion, as well as to improve the overall system performance [12], [15]. In this study we used an imaging receiver and two types of diversity schemes (select the best (SB) and maximum ratio combining (MRC)) to choose or add the received power collected by different pixels. A delay adaptation technique (DAT) for a VLC system was proposed in [12] and it is used here as it was shown to offer channel bandwidths of more than 36 GHz (in a worst case scenario), which enables the VLC system to operate at data rates of more than 20 Gbps. The adaptation techniques (LEA, BSR and DAT) require a repetitive training and feedback channel from the receiver to transmitter at a low data rate. An IR diffuse channel is suggested to achieve this channel. The ultimate goal of this work is to enhance the SNR at high data rates, reduce the effect of receiver mobility and

minimise delay spread (maximise channel bandwidth) within a realistic environment.

The VLC system model is described in the next Section. The receiver structure is given in Section III. Section IV describes the VLC system's configurations. The impact of beam steering on illumination is investigated in Section V. Adaptive finite vocabulary of holograms for VLC are considered in Section VI. The simulation results in an empty room are outlined in Section VII. Robustness against shadowing is evaluated in Section VIII. A high speed adaptive mobile VLC system is introduced in Section IX. Finally, conclusions are drawn in Section X.

II. VLC SYSTEM MODEL

A. Simulation environment

To evaluate our proposed techniques (LEA, BSR and DAT), a simulation was conducted in an empty room with dimensions of 4m×8m×3m (width × length × height). Experimental measurements of plaster walls have shown that they are roughly a Lambertian reflector [33]. Therefore, all the walls, the ceiling and the floor were modelled as Lambertian reflectors with high reflectivity (reflection coefficient of 0.3 for floor and 0.8 for walls and ceiling). These relatively high reflectivities (within the typical range) were selected as they result in the greatest multipath dispersion (worst case scenario), and consequently considerable pulse spread. Reflections from doors and windows were considered to be comparable to the reflections from the walls. To model the reflections, the room was divided into a number of equally sized squares with an area of dA and reflection coefficient of ρ. Each reflection element was treated as a small transmitter that transmitted an attenuated version of the received signals from its centre in a Lambertian pattern with $n=1$, where n is the Lambertian emission order.

Previous research considered only LOS and reflections up to a first order [3]-[8], [34]. However, this may not provide a full description of the characteristics of the system. Therefore, in this study reflections up to the second order were considered, since the second order reflections can have a great impact on the system performance at multi gigabits per second data rates [34].

In the practical VLC system, the impulse response is continuous, but the simulator subdivides the reflecting surfaces into discrete elements. We have tried to reduce the effect of discretisation by grouping power within a time bin of duration equal to 0.01 ns into a single received power. A good choice of time bin should be $\leq \sqrt{dA}/c$, which is roughly the time light takes to travel between neighbouring elements [35]. It should be noted that reducing dA leads to improved resolution in the impulse response evaluation together with an increase in the computation time exponentially. Surface elements of 5 cm × 5 cm for first-order reflections and 20 cm × 20 cm for second-order reflections were used. These values were selected to keep the computation requirements within a reasonable time (the computation time increases dramatically when the surface element size is decreased).

The room's illumination was provided by eight RGB-LDs light units that were used to ensure ISO and European standards were satisfied [36]. Each LD light unit has nine (3×3) RGB-LDs. The LD lights were installed at a height of 3m above the floor. The specifications of the RGB-LDs used in this study were adapted from the practical results reported in [9] where the measured illuminace for each RGB-LD was 193 lx. Therefore, the centre illumination intensity for each RGB-LD was 162 cd. The VLC room with the coordinates of the RGB-LDs light units is shown in Fig. 1. A number of different uniformly distributed LD light
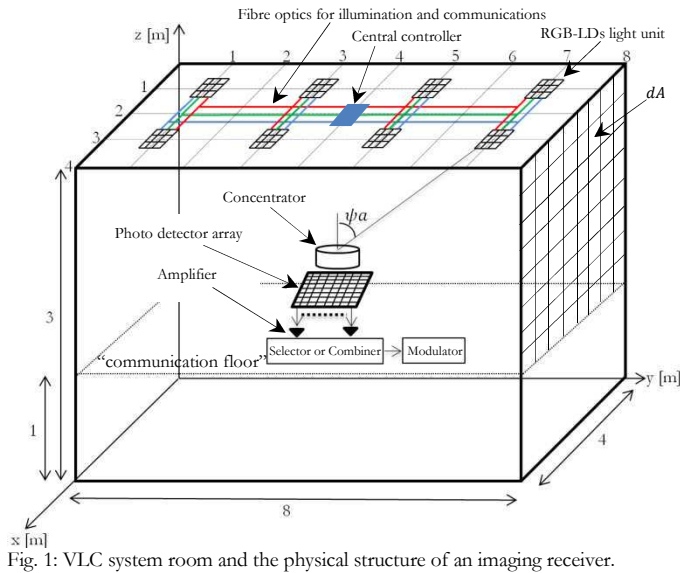
unit configurations (i.e. four, six and eight LD light units) were tested to find the optimum number of units that ensured the ISO and EU illumination requirements were satisfied in the room. We found that eight units were the optimum for illumination, and we used this in our study; four and six light units in the room did not achieve the minimum illumination requirement (i.e. 300 lx [36]) at all locations. The height of the work desks where the transmitters and receivers associated with the user equipment were placed was 1m. This horizontal plane was referred to as the "communication floor". The transmitted power from each RGB-LDs was 2 W. The simulations and calculations reported in this study were carried out using MATLAB. Our simulation tool was similar to the one developed by Barry et al. [35]. In our evaluation, the channel characteristics, optical power received, delay spread, 3 dB channel bandwidth and SNR calculations were determined in similar ways to those used in [10], [32], [37], [38]. Additional simulation parameters are given in Table I.

B. Channel characteristics of VLC system

In OW links including VLC channel, intensity modulation with direct detection (IM/DD) is the simplest modulation format and is as such used widely [37, 39]. The IM/DD channel can be modelled as a baseband linear system. In which $x(t)$ is the input power and $I(t)$ is the photo current received, which results from the integral of the received optical power over the photo detector surface. An indoor OW channel that uses IM/DD can be fully characterised by the impulse response of the channel as given in [40], [41]:

$$I(t) = Rx(t) \otimes h(t) + n_b(t) \qquad (1)$$

where R is the photo detector responsivity, t is the absolute time, $\otimes$ denotes convolution, n_b is the background noise (BN), which is modelled as AWGN, and $h(t)$ is the impulse response of the channel.

Fig. 1: VLC system room and the physical structure of an imaging receiver.

III. IMAGING RECEIVER

The imaging receiver is a good solution that can mitigate the impact of ISI and provide mobility for a VLC system [12]. Two significant advantages are offered by imaging receivers over non-imaging receivers: first, a single planner array is used for all photo-detectors, which can facilitate the use of a large number of pixels. Second, a common imaging concentrator (for example, a lens) can be shared between all photo-detectors, reducing the cost and size compared to other kinds of receivers. The detector array of the imaging receiver is segmented into j equal-sized

rectangular shaped pixels as shown in Fig. 1. In this case and under most circumstances, the signal falls on no more than four pixels [19]. We set the semi acceptance angle (ψ_a) of the concentrator to 65° so that it could view the whole ceiling when the receiver is at the centre of the room. In this work, the photo detector array of the imaging receiver is segmented into 50 pixels. When the receiver is at the centre of the room it is designed to see the whole ceiling, therefore the ceiling was subdivided, in this case, into 50 segments (5×10 along the x and y axes respectively), and each reception area or segment is cast onto a single pixel. The imaging receiver employed an imaging concentrator (lens) that could collect and concentrate the light from a large input area down to a smaller detector area (exit area). The transmission factor of the concentrator is given by [31]:

$$T_c(\delta) = -0.1982\delta^2 + 0.0425\delta + 0.8778 \qquad (2)$$

where δ is the incidence angle and is measured in radians. The lens has the parameters in [31] and in particular an entrance aperture with 3 cm diameter so that the an entrance area is $A = \frac{9\pi}{4}$ cm², an acceptance semi-angle of ψ_a=65°. When the reception angle δ exceeded ψ_a the concentrator transmission factor rapidly approached zero.

The detector array is assumed to fit exactly into its corresponding concentrator's exit area. Therefore, the detector array has a photosensitive area of 2 cm² and each pixel has an area of 4 mm². The pixel's reception area calculations are given in detail in [12]. The imaging receiver is always placed on the communication floor along the x=1m and x=2m lines (see Fig. 2). The imaging photo detector and concentrator sizes are acceptable for use with mobile devices. Each pixel in the imaging receiver has its own amplifier to amplify the received photocurrent (see Fig. 1). In our previous work, a simulation package based on a ray-tracing algorithm was developed to compute the impulse response for different VLC systems [12]-[15]. In this study, additional features were introduced to enable LEA, BSR and delay adaptation.

TABLE I
SIMULATION PARAMETERS

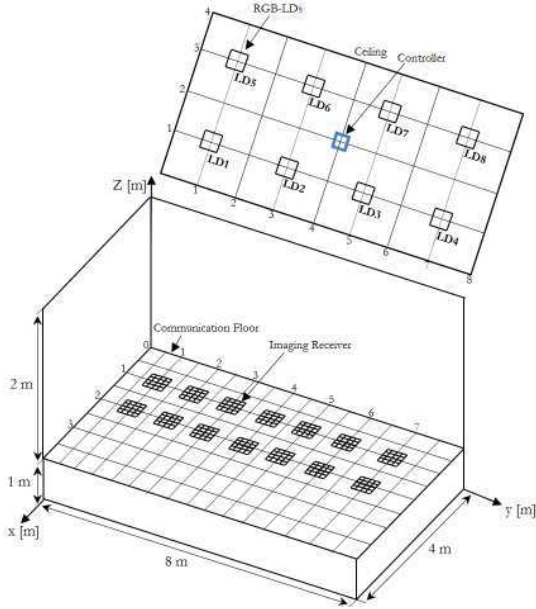| Parameters	Configurations	
Length	8m	
Width	4m	
Height	3m	
ρ-ceiling	0.8	
ρ-xz wall	0.8	
ρ-yz wall	0.8	
ρ-xz op-wall	0.8	
ρ-yz op-wall	0.8	
ρ-floor	0.3	
Bounces	1	2
Number of elements	32000	2000
dA	5cm×5cm	20cm×20cm
Transmitters		
Number of transmitters	8	
Locations	(1,1,3), (1,3,3), (1,5,3), (1,7,3)	
(x,y,z)	(3,1,3), (3,3,3), (3,5,3), (3,7,3)	
Elevation	90°	
Azimuth	0°	
Number of RGB-LDs per unit	9 (3×3)	
Semi-angle at half power	70°	
Centre luminous intensity	162 cd	
Transmitted optical power	2 W	
Imaging Receiver		
Quantity	1	
Detector array area's	2 cm²	
Number of pixels	50	
Pixel's area	4 mm²	
Elevation	90°	
Azimuth	0°	
Responsivity	0.4 A/W	
Time bin	0.01 ns	
Receivers bandwidth	30 MHz	20 GHz
Bit rates	30 Mbps	20 Gbps

Fig. 2: Imaging receiver test area locations on the communication floor.

At each pixel the received multipath profile from each RGB-LDs unit was computed, based on the area that the pixel observes and the pixel's FOV at each receiver location (fourteen different locations, see Fig. 2). Various parameters were derived from the simulated impulse response, such as the delay spread, 3 dB channel bandwidth and SNR.

1) Delay spread is a good measure of signal pulse spread due to the temporal dispersion of the incoming signal. The delay spread of an impulse response is given by [18]:

$$D = \sqrt{\frac{\sum(t_i-\mu)^2 P_{ri}^2}{\sum P_{ri}^2}} \qquad (3)$$

where t_i is the delay time associated with the received optical power P_{ri}, and μ is the mean delay given by:

$$\mu = \frac{\sum t_i P_{ri}^2}{\sum P_{ri}^2} \qquad (4)$$

2) The 3 dB channel bandwidth is equal to the frequency when the magnitude response falls by 3 dB.

3) The SNR of the received signal can be calculated by taking into account the powers associated with logic 0 and logic 1 (P_{S0} and P_{S1}) respectively. The SNR is given by [40]:

$$SNR = \left(\frac{R(P_{S1}-P_{S0})}{\sigma t}\right)^2 \qquad (5)$$

where R is the receiver responsivity (0.4 A/W) and σ_t is the standard deviation of the total noise, that is the sum of shot noise, thermal noise and signal dependent noise. The σ_t can be calculated as:

$$\sigma t = \sqrt{\sigma_{shot}^2 + \sigma_{preamplifier}^2 + \sigma_{signal}^2} \qquad (6)$$

where σ_{shot}^2 represents the background shot noise component, $\sigma_{preamplifier}^2$ represents the preamplifier noise component and σ_{signal}^2 represents the shot noise associated with the received signal. The detection of light by a photodiode is a discrete process since the creation of an electron-hole pair is dictated by the statistics of photon arrivals. The latter is a discrete process and obeys the Poisson distribution. The discrete nature of the photo-detection process creates a signal dependent shot noise, quantum noise. Quantum noise results from the random generation of electrons by the incident optical radiation [42].

The receivers used in this study and the values of the noise are similar to those in [12] and [15]. For the 20 Gbps system we used the pre-amplifier in [43]. In this study we considered two methods of processing the electrical signal (SB and MRC) from different pixels in an imaging receiver. In the SB the receiver simply selects the pixel with the largest SNR among all the pixels. The SNR_{SB} is given by [40]:

$$SNR_{SB} = Max_i \left(\frac{R(P_{S1}-P_{S0})_i}{\sigma t_i}\right)^2 \quad 1 \leq i \leq j \qquad (7)$$

where j represents the number of pixels (j=50 in our imaging receiver). In contrast to the SB, the MRC utilises all pixels from the imaging receiver. The output signals of all the pixels are combined through an adder circuit. Each input to the circuit is added with a weight proportional to its SNR to maximise the SNR [44]. The signals from all pixels (j) are combined using weights equal to W_i. It can be shown that the SNR of the MRC is maximum when the weight factor at the receiver pixel is chosen to be proportional to each pixel's signal-to-noise-variance ratio [31], where $W_i = \left(\frac{R(P_{S1}-P_{S0})}{\sigma_t^2}\right)_i$. One of the main advantages of the MRC scheme is that it reduces the dominant effect of background shot noise by assigning a low W_i value to the pixel that is most severely affected by background noise, hence improving the system performance. The SNR_{MRC} is given by:

$$SNR_{MRC} = \frac{\left(\sum_{i=1}^j R(P_{S1}-P_{S0})_i W_i\right)^2}{\sum_{i=1}^j \sigma_{t_i}^2 W_i^2} \qquad (8)$$

By substituting (W_i) in (8), the SNR obtained using MRC combining method is given by: $SNR_{MRC} = \frac{\left(\sum_{i=1}^j R(P_{S1}-P_{S0})_i \left(\frac{R(P_{S1}-P_{S0})}{\sigma_t^2}\right)_i\right)^2}{\sum_{i=1}^j \sigma_{t_i}^2 \left(\frac{R(P_{S1}-P_{S0})}{\sigma_t^2}\right)_i^2}$

$$= \frac{\sum_{i=1}^j R^2 (P_{S1}-P_{S0})_i^2 \left(\frac{R(P_{S1}-P_{S0})}{\sigma_t^2}\right)_i^2}{\sum_{i=1}^j \sigma_{t_i}^2 \left(\frac{R(P_{S1}-P_{S0})}{\sigma_t^2}\right)_i^2} = \sum_{i=1}^j \frac{(R(P_{S1}-P_{S0})_i)^2}{\sigma_{t_i}^2} = \sum_{i=1}^j SNR_i \qquad (9)$$

IV. VLC SYSTEMS CONFIGURATIONS

In this section, four VLC systems are presented, analysed and compared to identify the most appropriate system for use in high-speed VLC systems (20 Gbps and beyond).

A. Imaging LDs-VLC system

The imaging LDs-VLC system employed eight RGB-LDs transmitters (lighting fixtures) on the ceiling connected by fibre interconnect and controlled by a central controller and an imaging receiver with 50 pixels. The imaging LDs-VLC system was proposed in [12] and it is considered here to compare it with our new proposed VLC systems.

B. DAT imaging LDs-VLC system

The DAT imaging LDs-VLC system has a similar configuration as the previous system. However, the delay adaptation technique is combined with imaging LDs-VLC (DAT imaging LDs-VLC) to enhance the overall system performance. The DAT imaging LDs-VLC system was previously proposed in [12].

C. Beam steering LDs-VLC system

The newly proposed beam steering LDs-VLC system has a similar room configuration and uses the same transmitters and receiver as in the previous systems. However, three new algorithms were introduced to enable the system to achieve data rates higher than 10 Gbps. Select-the-best (STB), LEA and BSR algorithms were used to enhance the SNR of the new VLC system.

D. Fully adaptive VLC system

In contrast to the beam steering LDs-VLC system, the fully adaptive VLC system employed a finite vocabulary of stored

4

holograms to reduce the computation time required by LEA to identify the best location of beam steering and using the delay adaptation technique to further improve the communication link performance. In contrast to our previous work in [12]-[15] where the RGB-LDs light unit had a fixed form pattern, we propose here a fully adaptive VLC system where the transmitter (RGB-LDs light unit) has the ability to direct part of the white light towards the receiver location to enhance the SNR when operating at high data rates.

LEA and BSR were implemented in a certain RGB-LDs light unit for a single receiver at a given set of positions; when the receiver starts moving, they are applied in another RGB-LDs light unit according to the new receiver location (coordinates). The SNR improvement at high data rates (i.e. 20 Gbps) could be achieved according to the following algorithms:-

❖ STB algorithm is proposed to locate the closest transmitter (RGB-LDs) to the receiver to implement LEA and BSR. The STB algorithm identifies the closest transmitter to the receiver according to the following steps:
  1) A pilot signal is sent from one of the VLC transmitters.
  2) The SNR is estimated at the receiver by pixel 1 of the imaging receiver.
  3) Repeat step 2 for the other pixels in the imaging receiver.
  4) Repeat steps 2 and 3 for the other VLC transmitter units.
  5) The receiver sends (using an infrared beam) a low data rate control feedback signal to inform the controller of the SNRs associated with each transmitter.
  6) The transmitter that yields the best SNR is chosen by the controller (typically the closest transmitter to the receiver in our simulations).

It should be noted that the RGB-LDs light units should always be 'ON' to provide illumination for the room. Therefore, to prevent flickering, a pulse width modulation (PWM) dimming technique may be used [45]. The information signals are coded (each RGB-LDs unit has its own code) and sent from each RGB-LDs light unit by the central controller. Once the receiver receives the coded signal from the RGB-LDs light unit, the SNR is computed and a feedback signal is sent. If the time taken to calculate the value of each SNR with each RGB-LDs unit is equal to 1 ms (based on typical processor speeds) then the STB algorithm training time is 8 ms (8 RGB-LDs units × 1 ms).

❖ A new LEA is introduced to the VLC system to identify the optimum location to carry out optical BSR. The RGB-LDs light unit that has been chosen in the STB algorithm initially produces a single beam using a SLM and scans it along a number of possible locations in the room to identify the location of the receiver. At each beam setting the receiver computes the SNR and the optimum beam location is selected at the controller. The location estimation algorithm is an effective approach that can help identify the optimum direction for BSR in a way that gives the best SNR at the receiver.

The RGB-LDs light unit is followed by the SLM that generates beams whose locations can be varied where the transmission angles θ_x and θ_y in the xy axes are varied between -70° and 70° (half power beam angle of RGB-LDs light unit was 70°) with respect to the transmitter's normal in both the x and the y (α_{-x} to α_x and α_{-y} to α_y) directions respectively. The LEA produces a single beam and scans it with step angle (β) along a range of rows and columns in the room to identify the location that yields the best receiver SNR based on a divide and conquer (D&C)

algorithm. The coordinates of this location are used as the centre of the BSR direction. β is chosen to be large in the first iteration (26.56°, which allows the spot to move 100 cm) to reduce the number of locations that have to be scanned. The angle is then reduced by a factor of two in each following iteration. The position that results in the best SNR is identified as a sub-optimum location, and the quadrant that includes this sub-optimum location is selected as a new scanning area for the next iteration. A number of iterations are carried out until the final optimum location is identified (eight scan iterations are considered to achieve β=0.28° or step size of 1 cm). LEA scans 224 possible locations in eight iterations until reaching the target step size (1 cm). LEA determines the two transmission angles θ_x and θ_y that identify the coordinates (x, y, z) of the best SNR location according to the following steps:
  1) Configure the RGB-LDs light unit to implement scan locations according to the associated parameters: the x-axis scan range (θ_x^{Start} to θ_x^{End}), the y-axis scan range (θ_y^{Start} to θ_y^{End}) and the step angle (β). A single beam is moved by changing the beam angles between -70° and 70° in steps of β to determine the sub-optimum location. Some of the scan points will be on the walls due to the RGB-LDs light unit's position, as shown in Fig. 3.
  2) The SNR is computed at each step and the receiver sends a control feedback signal at a low rate to inform the controller of the SNR associated with each scan. This feedback channel can be implemented using an infrared beam.
  3) Compare the SNR computed and recorded with the associated transmission angles θ_x and θ_y that give the maximum SNR.
  4) Determine the sub-optimum coordinates (x_s, y_s, z_s) of the beam that produces the sub-optimum SNR based on its transmission angles θ_x and θ_y.
  5) To configure the next iteration, the controller identifies the quadrant that includes the sub-optimum location from θ_x and θ_y and assigns it as the boundary angles of the new scanning area (α_{-x} to α_x and α_{-y} to α_y).
  6) The new scanning area is divided into four quadrants and β is reduced by a factor of two.
  7) Repeat steps 1 to 4 to identify the best location that gives the highest SNR. The iterations stop when $\beta \leq$ 0.28° (beam step is 1 cm).
  8) The controller assigns the optimum location with the coordinates (x, y, z) to the transmitter.

❖ The new BSR technique focuses a part of the light of one of the RGB-LDs towards the coordinates that were found by the LEA algorithm. According to the illumination results, which will be discussed in the next section, up to 20% of the RGB-LDs light unit can be beam steered towards the receiver's location while the remaining white light (i.e. 80%) is used for illumination.

The adaptation techniques (LEA, BSR and DAT) require a repetitive training and feedback channel from the receiver to transmitter at a low data rate. An IR diffuse channel is suggested to achieve this channel. An IR sensor is attached to the RGB-LDs light unit. Heat sources such as RGB-LDs light unit may negatively affect the performance of the feedback channel (IR diffuse) as they may be considered as interference sources [46]. However, it should be noted that in this work we have used the

RGB-LDs light units which have lower heat emission than conventional lamps such as halogen or incandescent. In addition, the main function of this channel is to send a feedback signal and the data rates used in this channel are very low (i.e. tens of kbps). Therefore, the effect of heat sources is very small and may be neglected. Fig. 4 shows a block diagram of the transmitter and receiver with uplink and downlink channels. The SLM in the transmitter is used for beam steering, and it is a transparent or reflective device that is used to spatially modulate the phase or amplitude of each pixel [47]. The SLM can operate as a dynamic diffractive convex lens when the Fresnel lens function is applied by using the control electronic signal [22]. The SLM devices have µs to ms response times that are sufficient to carry out the BSR technique at the rate of mobile receiver movements [48]. The SLM and control circuit can generate beams to scan the communication floor and estimate the receiver location (see Fig. 5). Changing the holographic function through the control circuit can generate variable optical beam locations on the communication floor with different switching times. Once, the beam steering technique is applied, delay adaptation can be utilised to reduce the effect of multipath and reduce the delay spread (increase channel bandwidth). An imaging receiver employing narrow FOV pixels can be used to mitigate the effect of multipath propagation due to the limited range of rays received. However, it has been seen in a VLC system that the delay spread is influenced by the RGB-LDs spots' relative positions and the number of RGB-LDs spots seen by the FOV of each pixel [12]. Thus, emitting signals from all RGB-LDs units at the same time may cause a time delay differential between the signals received at the pixel, which results in spreading the received pulse and hence limiting the bandwidth.
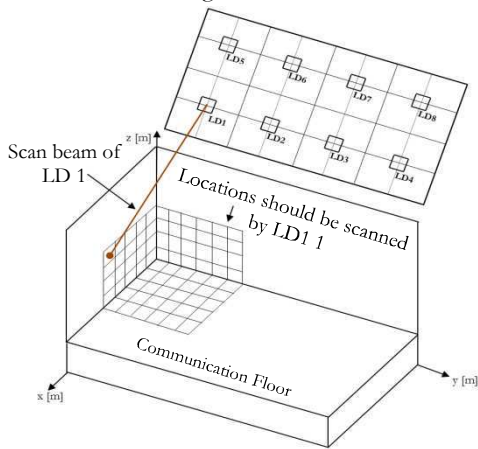

Fig. 3: LEA implemented at one of the corner RGB-LDs light units.

Fig. 4: Block diagram of the fully adaptive VLC system.

Therefore, instead of sending the signals at the same time from different LD light units, the delay adaptation algorithm sends the signal that has the longest journey first, and then sends the other signals with different differential delays (Δt) so that all the signals reach the receiver at the same time. The delay adaptation algorithm for a VLC system was proposed in [12], and it is used here to offer improvements in terms of bandwidth efficiency. The delay adaptation can be implemented through array elements delayed switching. The delay adaptation adjusts the switching times of the signals as follows:

1) A pilot signal is sent from the first transmitter.
2) The mean delay (μ) at the receiver for the first lighting unit is estimated at the receiver side by pixel 1 of the imaging receiver.
3) Repeat step 2 for the other pixels in the imaging receiver.
4) Repeat steps 2 and 3 for the other VLC transmitter units.
5) The receiver sends a control feedback signal to inform the controller of the associated delay with each received signal from each transmitter.
6) The controller introduces a differential delay (Δt) between the signals transmitted from the transmitters.
7) The transmitter units send signals according to the delay values, such that a transmitter unit that has the largest delay, i.e. longest path to the receiver, transmits first.
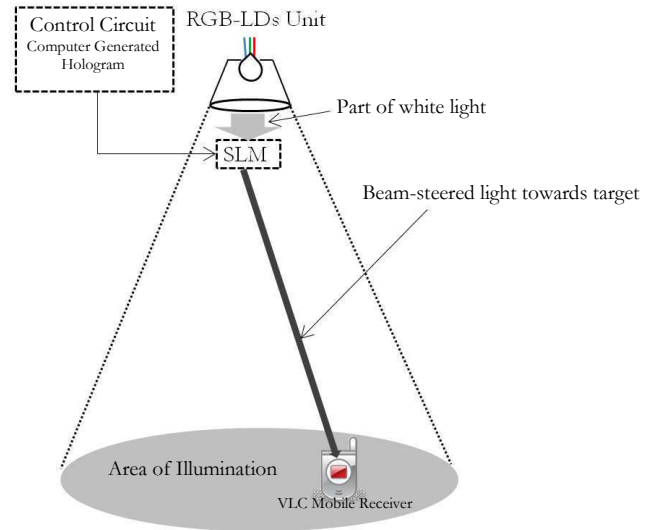

Fig. 5: Beam steering technique applied at one of the RGB-LDs light unit.
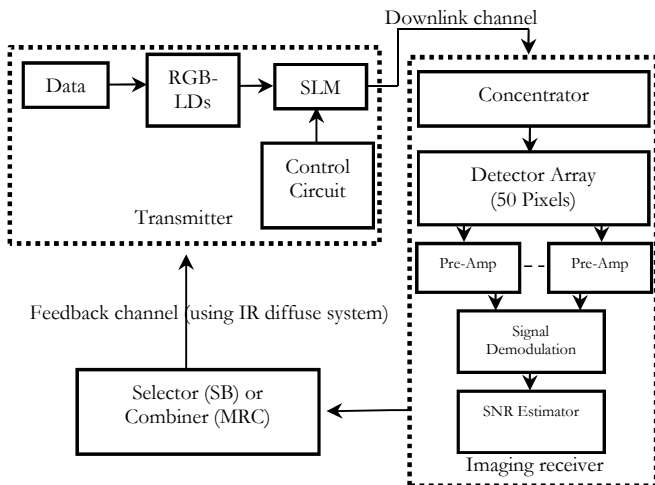
A pedestrian user moves indoor at a speed of about 1 m/s [49]. We therefore propose that the receiver re-estimates its SNR and delay values for all RGB-LDs light units at the start of a one second frame, and if these have changed compared to the previous frame's values then the receiver uses the feedback channel to update the controller. If the time taken to determine the value of each SNR and delay associated with each transmitter (relative to the start of the frame) is equal to 1 ms (based on typical processor speeds), then LEA and the delay adaptation method training time will be 296 ms (224 possible locations should be scanned in all iterations × 1 ms + 9 RGB-LDs in each transmitter unit × 8 transmitter units × 1 ms). This time (296 ms, once every one second frame) is sufficient given that LEA and delay adaptation have to be carried out at the rate at which the environment changes (pedestrian movement). Therefore, the beam steering LDs-VLC system can achieve 100% of the

6

specified data rate when it is stationary, and 70.4% in the case of user movement, (user or object movement in the room). LEA, BSR and delay adaptation algorithms are carried out at one given receiver location for the single user scenario to enhance the SNR and bandwidth at the receiver, and this can be achieved through the algorithms given in Fig. 6. In the case of a multiple users scenario, opportunistic scheduling [50] can be used where LEA, BSR and delay adaptation algorithms are implemented opportunistically (or randomly between users/regions) to maximize the 3 dB channel bandwidth and the SNR in a given region for a given time period. The MAC protocol should include a repetitive training period to perform the algorithms in Fig. 6. The design of the MAC protocol is not considered in this work.
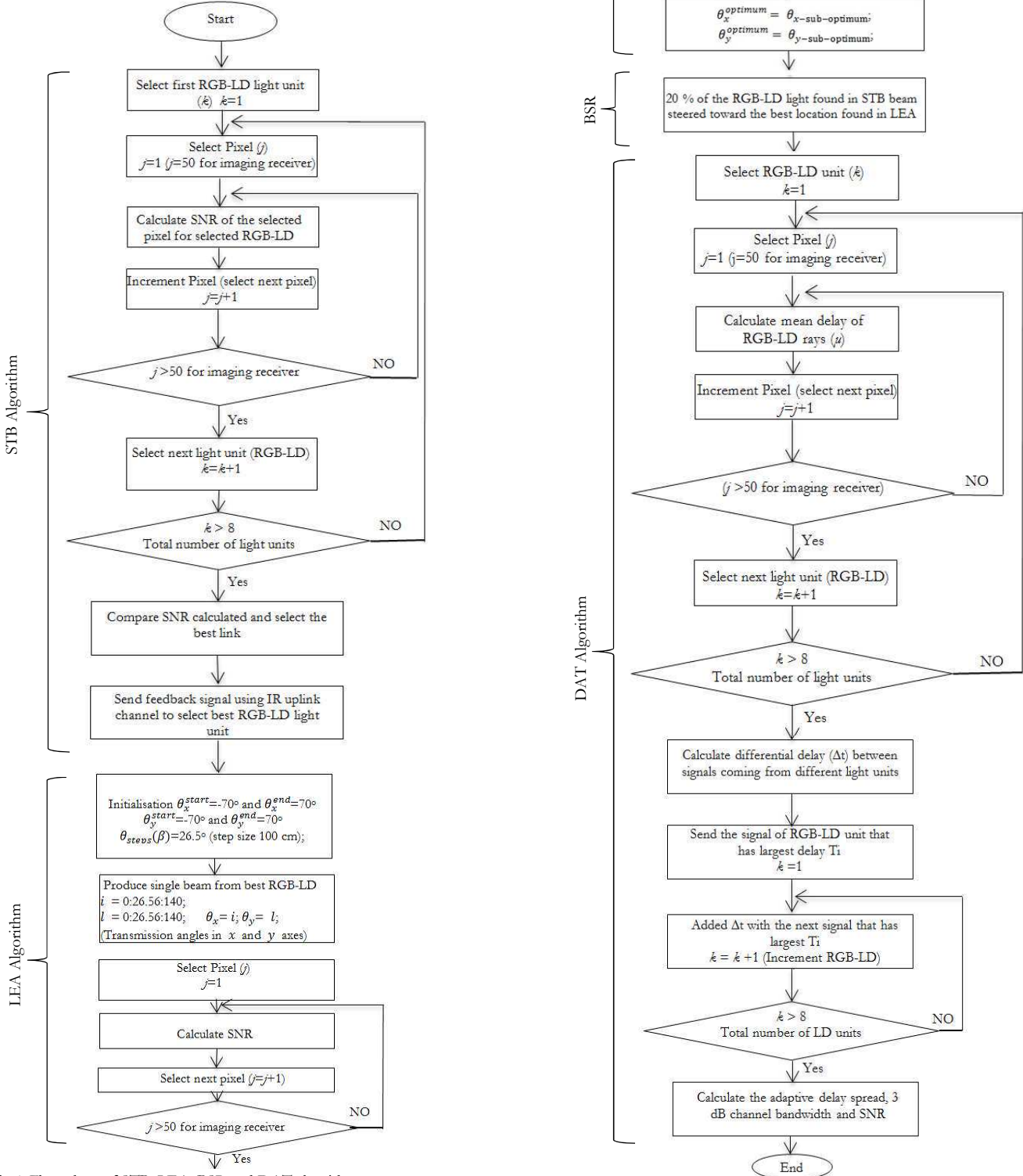
STB Algorithm

Start

Select first RGB-LD light unit (k) $k=1$

Select Pixel (j) $j=1$ ($j=50$ for imaging receiver)

Calculate SNR of the selected pixel for selected RGB-LD

Increment Pixel (select next pixel) $j=j+1$

$j>50$ for imaging receiver — NO

Yes

Select next light unit (RGB-LD) $k=k+1$

$k>8$ Total number of light units — NO

Yes

Compare SNR calculated and select the best link

Send feedback signal using IR uplink channel to select best RGB-LD light unit

LEA Algorithm

Initialisation $\theta_x^{start}=-70°$ and $\theta_x^{end}=70°$
$\theta_y^{start}=-70°$ and $\theta_y^{end}=70°$
$\theta_{steps}(\beta)=26.5°$ (step size 100 cm);

Produce single beam from best RGB-LD
$i = 0:26.56:140$;
$l = 0:26.56:140$; $\theta_x= i$; $\theta_y= l$;
(Transmission angles in x and y axes)

Select Pixel (j) $j=1$

Calculate SNR

Select next pixel ($j=j+1$)

$j>50$ for imaging receiver — NO

Yes

Fig.6: Flow chart of STB, LEA, BSR and DAT algorithms.

LEA Algorithm (cont.)

$SNR (i, l) = \max(SNR_j)$

$pixel (i, l) = find (SNR_j) == (\max (SNR_j))$;

Identify sub-optimum location

Set new values for θ_x and θ_y and start another iteration

Stop iterations when $\beta \leq 0.28°$ — NO

Yes

$\theta_x^{optimum} = \theta_{x-\text{sub-optimum}}$;
$\theta_y^{optimum} = \theta_{y-\text{sub-optimum}}$;

BSR

20 % of the RGB-LD light found in STB beam steered toward the best location found in LEA

DAT Algorithm

Select RGB-LD unit (k) $k=1$

Select Pixel (j) $j=1$ ($j=50$ for imaging receiver)

Calculate mean delay of RGB-LD rays (μ)

Increment Pixel (select next pixel) $j=j+1$

($j>50$ for imaging receiver) — NO

Yes

Select next light unit (RGB-LD) $k=k+1$

$k>8$ Total number of light units — NO

Yes

Calculate differential delay (Δt) between signals coming from different light units

Send the signal of RGB-LD unit that has largest delay Ti $k =1$

Added Δt with the next signal that has largest Ti $k = k +1$ (Increment RGB-LD)

$k>8$ Total number of LD units — NO

Yes

Calculate the adaptive delay spread, 3 dB channel bandwidth and SNR

End

V. THE IMPACT OF BEAM STEERING TECHNIQUE ON ROOM ILLUMINATION

The main function of the RGB-LDs light units is to provide sufficient illumination according to ISO and European standards [36]. Therefore, to ensure the illumination is at an acceptable level we controlled the white light directed towards the receiver so that only a small amount of the RGB-LDs light is beam steered towards the receiver (20% of light of RGB-LDs unit), and the remaining light is used for illumination. We examined different values of light beam steering (10%, 20% and 30%) and we found that 20% achieves good performance in terms of the improvement in the achievable channel bandwidth and data rate while obeying the illumination standards with an acceptable change in illumination (i.e. the reduction in illumination is within the threshold level of European standards, which is 300 lx).

Fig. 7 shows the horizontal illumination distribution for the eight RGB-LDs units, the comparison is carried out for the illumination with and without beam steering when 10%, 20% and 30% of the beam power is steered, applied at LD1 (see Fig. 2 for RGB-LDs numbers and locations). The LD1, LD4, LD5 and LD8 light units were located at the room corners, and when beam steering of more than 20% is carried out at one of these light units, this led to reduced illumination in the room corners that is less than the threshold level (i.e. less than 300 lx, see Fig. 7c). The minimum illumination in the corner without beam steering was 336 lx, as shown in Figs. 7 (a), (b) and (c). However, when beam steering was applied at one of the corner RGB-LDs units (worst case scenario) the illumination decreased, due to a part of the RGB-LDs' light being steered towards the receiver location (e.g. at 1m, 1m, 1m). The minimum illumination values of 10%, 20% and 30% beam steering were 323 lx, 300 lx and 275 lx respectively. Therefore, we chose 20% beam steering as an acceptable value that kept the illumination at an acceptable level (300 lx) and improved the SNR. We emphasise that the beam steering technique is carried out at one RGB-LDs light unit that is nearest to the receiver location (the RGB-LDs that has been chosen by the STB), while the remaining RGB-LD light units (seven RGB-LD light units) operate normally. Note that steering light to a receiver, not only increases the received power, it more importantly reduces the delay spread by increasing the power received through the direct ray well beyond the power received through reflections.
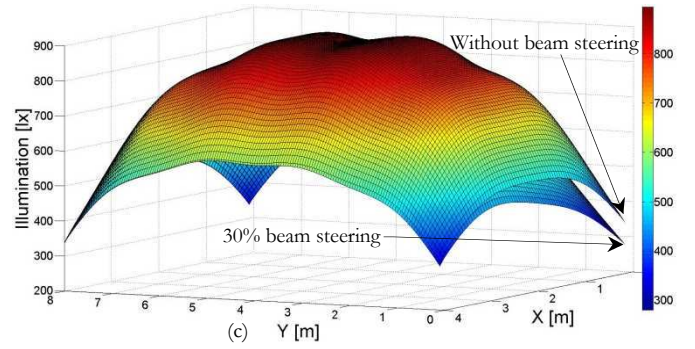

Fig. 7: The distribution of horizontal illumination on the communication floor without beam steering minimum illumination 336lx and maximum illumination 894lx: (a) 10% beam steering minimum illumination 323 lx and maximum illumination 892 lx (b) 20% beam steering minimum illumination 300 lx and maximum illumination 889 lx (c) 30% beam steering minimum illumination 275 lx and maximum illumination 887 lx.
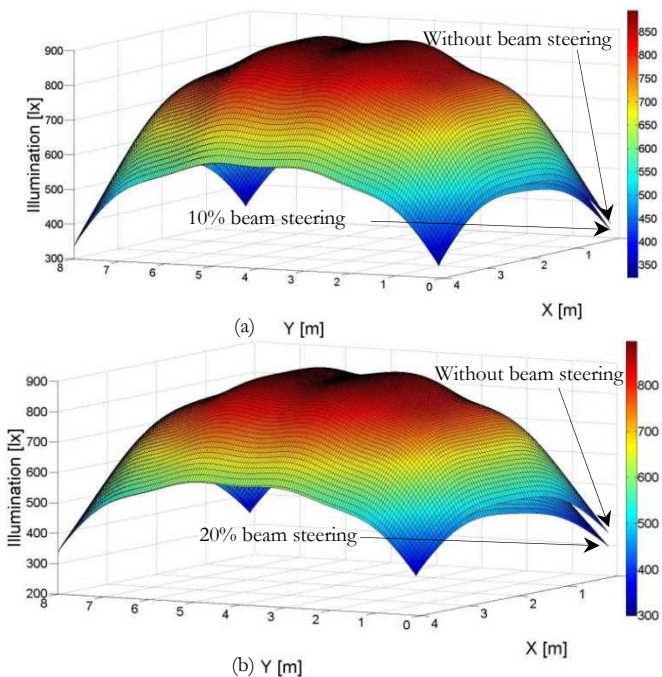
VI. ADAPTIVE FINITE VOCABULARY OF HOLOGRAMS FOR VLC

An angle and power adaptive IR-OW system has recently been introduced [18], [19]. Beam angle adaptation for VLC systems can be an effective technique that helps to provide the strongest path between the transmitter and the receiver at every receiver location. The adaptive transmitter first produces a single spot to scan the communication floor at approximately 224 possible locations (associated with a 0.28° beam angle increment) in order to identify the best location. Once the optimum angles are found, the transmitter generates the hologram. These processes require intensive calculations and time from a digital signal processor (DSP). In order to eliminate the need to compute the beam steering holograms at each step to identify the best location, a new adaptation method is introduced here where a finite vocabulary of stored holograms is used. The floor ($2 \text{ m} \times 2\text{m}$) under the visible light sources is subdivided into small area i.e., 400 regions ($0.1 \text{ m} \times 0.1\text{m}$ per region), see Fig. 8. This large number of regions has been selected based on our recent optimization in [27], [28]. In each region, the transmitter uses a hologram that generates the optimum pattern if the receiver is present in any one of the regions. These holograms can be pre-calculated so as to target the spots near the receiver (in whichever region the receiver may be) based on LEA. Computer generated holograms (CGH) can produce spots with any prescribed amplitude and phase distribution. The CGH's have many useful properties. Spot distributions can be computed on the basis of diffraction theory and encoded into a hologram. Calculating a CGH means the calculation of its complex transmittance. The transmittance is expressed as:

$$H(u, v) = A(v, u). exp[j\phi(u, v)] \qquad (10)$$

where $A(u, v)$ is the hologram's amplitude distribution, $\phi(u, v)$ is its phase distribution, and (u, v) are coordinates in the frequency space. The relative phases of the generated spots are the objects of interest. The hologram is able to modulate only the phase of an incoming wave front, the transmittance amplitude being equal to unity. The analysis used in [27], [28], [51] was used for the design of the CGHs. The hologram $H(u, v)$ is considered to be in the frequency domain. The pixels' locations in the hologram are defined by the frequency coordinates u and v (two dimensions). The observed diffraction pattern $h(x, y)$ is in the spatial domain (far field). They are related by the continuous Fourier transform:

$$h(x, y) = \iint H(u, v)exp[-i2\pi(ux + vy)]dudv \qquad (11)$$

8

The hologram structure is an $M \times N$ array of rectangular cells, with dimension $R \times S$. Each cell represents a complex transmittance value H_{kl}: $-M/2 < k < M/2$ and $-N/2 < l < N/2$. If the hologram is placed in the frequency plane, the diffraction pattern is given by [28], [52]:

$$h(x, y) = RSsinc(Rx, Sy) \sum_{k=-\frac{M}{2}}^{\frac{M}{2}-1} \sum_{l=-\frac{N}{2}}^{\frac{N}{2}-1} H_{kl} \, exp[i2\pi(Rkx + Syl)] \quad (12)$$

where $sinc(a,b) = sin(\pi a) \, sin(\pi b)/\pi^2 ab$. The hologram is designed such that the complex amplitude of the spots is proportional to some value of interest. However, because of the finite resolution of the output device and the complex transmittance of the resulting hologram, the reconstruction will be in error. This error can be used as a cost function. Simulated annealing was employed to minimize the cost function. The amplitudes and phases of every spot are determined by the hologram pixels' pattern and are given by its Fourier transform.

Fig. 8: VLC communication architecture of our proposed system when the transmitter is placed at (1m,1m,3m) and the receiver is at (1m,1m,1m).

The desired distribution of spots in the far field is $f(x,y) = |f(x,y)| exp(i\varphi(x,y))$. The main goal of the design is to determine the CGH distribution $g(v, u)$ that generates a reconstruction $g(x,y)$ as close as possible to the desired distribution $f(x, y)$. The cost function (CF) is defined as a mean squared error which can be interpreted as the difference between the normalized desired object energy $f''(x, y)$ and the scaled reconstruction energy $g''(x,y)$:

$$CF_k = \sqrt{\sum_{i=1}^{M} \sum_{j=1}^{N} (|f''(i,j)|^2 - |g''_k(i,j)|^2)^2} \quad (13)$$

where $f''(x, y)$ represents the normalized desired object energy and $g''_k(i, j)$ represents the scaled reconstruction energy of the kth iteration. Simulated annealing was used to optimize the phase of the holograms offline by minimizing the cost function.

For a large room of $8m \times 4m$, the floor is divided into 8 regions $(2 m \times 2m)$. Each region is subdivided into 400 small areas $(0.1 m \times 0.1m$ per area). A library that contains 100 holograms optimized offline using simulated annealing was established. A large number of holograms are required in order to accurately identify the receiver location within the region [28]. Each hologram produces the optimum pattern which was pre-calculated based on the LEA. Each region related to a particular visible light source in the ceiling, the VLC source should have 100 holograms stored in a library in order to cover the 400 possible receiver positions in the region. An example of one hologram, when the transmitter is placed in the corner of room

at: (1m, 1m , 3m) and the receiver is present at (1m, 1m, 1m), as shown in Fig. 8. Simulated annealing was used to optimize the phase of the computer-generated hologram. Fig. 9 shows three snapshots of hologram phase distributions, $g(x,y)$, in the far filed at different iterations. When the number of iterations increases, the hologram phase distributions improve. The cost function versus the number of iterations completed is shown in Fig. 10.

Hologram phase distributions (iteration 5)

Hologram phase distributions (iteration 15)

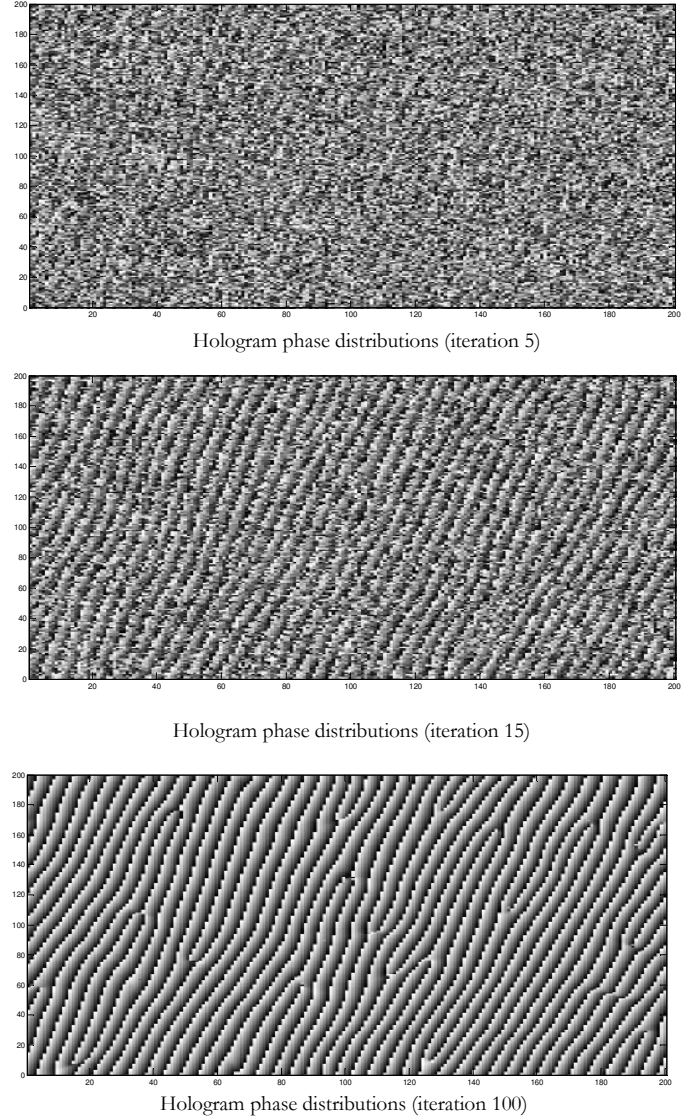
Hologram phase distributions (iteration 100)

Fig. 9: The hologram phase pattern at iterations 5, 15 and 100 using simulated annealing optimization. Different gray levels represent different phase levels ranging from 0 (black) to 2π (white).
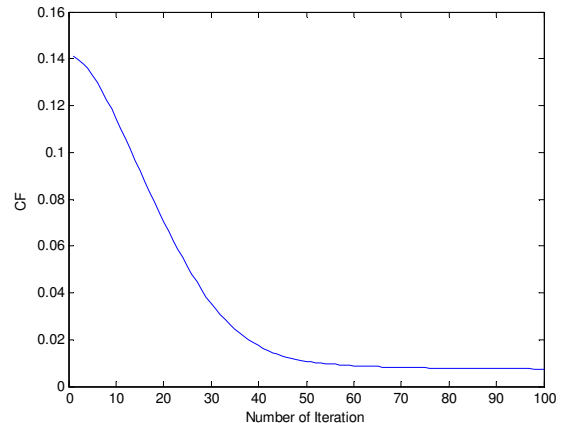

Fig. 10: Cost function versus the number of iterations.

VII. SIMULATION RESULTS AND PERFORMANCE ANALYSIS

In this section, we evaluate the performance of LEA, BSR and delay adaptation techniques in the presence of multipath propagation, ISI and mobility of the VLC system in an empty room. Two new VLC systems, beam steering LDs-VLC and fully adaptive LDs-VLC, were compared with imaging LDs-VLC and DAT imaging LDs-VLC. The results are presented in terms of impulse response, delay spread, 3 dB channel bandwidth and SNR.

A. Impulse responses

The impulse responses of the four VLC systems: imaging LDs-VLC, DAT imaging LDs-VLC, beam steering LDs-VLC and fully adaptive LDs-VLC, at the room centre are depicted in Fig. 11. The LOS components have a great impact on the system performance; therefore, we magnified the impulse responses for these systems to show the LOS contributions clearly. First and second order reflection components exist in the original impulse response, but they do not appear in this figure due to magnification of the LOS components. It can be clearly seen that the systems that employ the delay adaptation technique (DAT imaging LDs-VLC and fully adaptive) are significantly better than the other systems (imaging LDs-VLC and beam steering LDs-VLC) in terms of signal spread (recall that there are multiple VLC light sources in the room). The imaging LDs-VLC system (black line) produces 6.68 µW received power with a much greater signal spread due to sending the signals at the same time from different LD light units. A considerable reduction in the signal spread is observed when the delay adaptation technique is adopted in the imaging the LDs-VLC system as shown in blue line Fig.11. However, there is no increase in the amount of received optical power (the sum of received power is the same in both systems in imaging LDs-VLC and DAT imaging LDs-VLC). On the other hand, a significant increase in the received optical power can be achieved when the beam steering LDs-VLC system replaces the DAT imaging LDs-VLC system, by a factor of 7, from 6.68 µW to 47.46 µW, as shown in red line Fig. 11. This significant improvement in the received power is due to steering a beam of white light towards the receiver location. However, signal spread still exists in this system, and this lead to degradation in the system performance at high data rates. It can be clearly seen that the fully adaptive LDs-VLC system's impulse response is better than the other systems in terms of signal spread and received optical power, as shown in Fig. 11 compared to other systems. Reducing the signal spread of the beam steering LDs-VLC system leads to an increase in the 3 dB channel bandwidth that enables higher throughput for the VLC system and decreases the ISI caused by multipath.

B. Delay spread

Fig. 12 evaluates the delay spread of the four systems under the worst case scenario (when the receiver moves along x=2m). The middle of the room (x=2m) is considered to be the worst communication link in the communication floor area due to its associated high ISI and multipath propagation level; therefore, we only consider the x=2m line. The delay spread for the imaging LDs-VLC system is relatively low (0.04 ns in the worst case) and this is due to the narrow FOVs associated with each pixel in the imaging receiver, and this limitation in the FOV minimises the number of rays accepted. However, to operate at high data rates (10 Gbps and beyond) the delay spread should be further reduced (i.e. less than 0.04 ns). To improve the quality of the link we combined the delay adaptation technique with imaging LDs-VLC system.
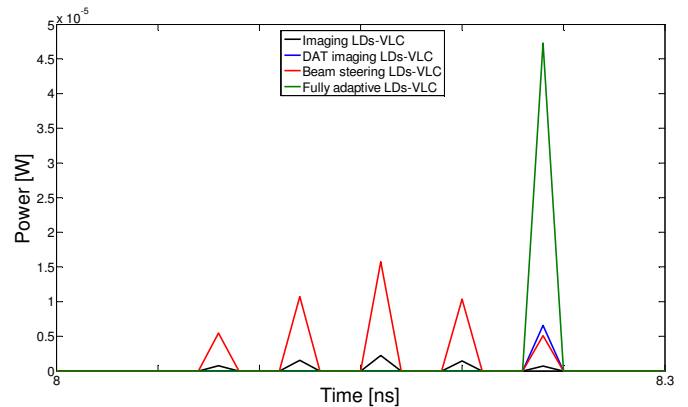

Fig. 11: Impulse responses of different VLC systems at room centre: laser diodes transmitters with an imaging receiver (imaging LDs-VLC), delay adaptation technique with laser diodes transmitters and imaging receiver (DAT imaging LDs-VLC), location estimation and beam steering techniques with laser diodes transmitters and imaging receiver (beam steering LDs-VLC) and location estimation, beam steering, delay adaptation, CGHs with laser diodes transmitters and imaging receiver (fully adaptive LDs-VLC).

The DAT imaging LDs-VLC system outperforms the imaging LDs-VLC system, as it dramatically decreases the delay spread from 0.04 ns to 0.007 ns (by a factor of 5) at the room centre. The beam steering LDs-VLC system has a slightly lower delay spread (0.036 ns at the room centre) compared to the imaging LDs-VLC system and this is due to the advantage of beam steering, which increases the amplitude of the LOS components (see Fig. 11) and this makes this LOS component dominant compared to the first and second order reflections. Moreover, the DAT imaging LDs-VLC system performs better than the beam steering system in terms of delay spread. This is due to the signal spread in the beam steering system, as shown in Fig. 11. Thus, to further enhance the performance of the beam steering system we combined the delay adaptation technique with beam steering to produce a fully adaptive VLC system that has the lowest delay spread reported to date to the best of our knowledge (0.0035 ns in the worst case scenario) compared with other systems. The results show that the fully adaptive system reduces the delay spread by a factor of 13 compared with the imaging LDs-VLC system (from 0.04 ns to 0.0035 ns) at the room centre. The receiver's locations of y=2m, 4m and 6m in the non-adaptive systems (imaging LDs-VLC and beam steering LDs-VLC) in Fig. 12 are considered to be the worst receiver locations (due to high multipath propagation). However, by employing the delay adaptation approach, these locations become better than other locations (y=1m, 3m, 5m and 7m) due to the ability of this delay adaptation method to reduce the effect of multipath propagation to the lowest level.

C. 3 dB channel bandwidth

Previous work [12], [15] has shown that delay adaptation with an imaging receiver can provide a 3 dB channel bandwidth of more than 16 GHz under the worst case scenario. However, the main problem with such a system is the low SNR at high data rates (10 Gbps and beyond). Therefore, to enable it to operate at 20 Gbps we proposed the beam steering technique to enhance the SNR at high data rates and to utilise the significant increase in the channel bandwidth that will enable our proposed system (fully adaptive VLC system) to operate at 20 Gbps. The 3 dB channel bandwidth at x=2m in our four systems is given in Table II. The results show that the fully adaptive VLC system has the ability to offer a communication channel with 3 dB bandwidth greater than 36 GHz.
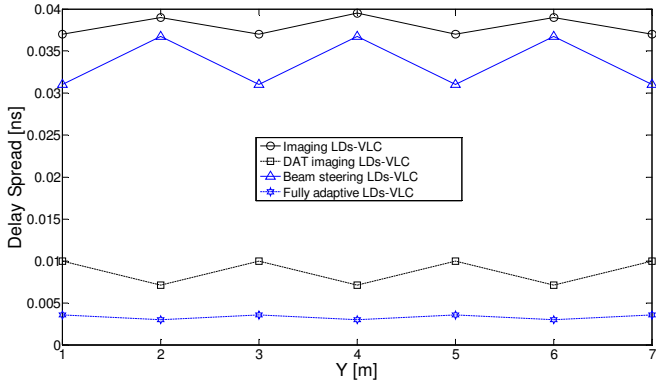
Fig. 12: Delay spread of four systems at x=2m and along the y-axis.

TABLE II
3 dB CHANNEL BANDWIDTH OF THE PROPOSED SYSTEMS

System	3 dB Channel Bandwidth [GHz]						
	Receiver Locations along the y-axis, y [m]						
	1	2	3	4	5	6	7
Imaging LDs-VLC	5.1	4.19	5.1	4.19	5.1	4.19	5.1
DAT Imaging LDs-VLC	16.6	23.4	16.6	23.4	16.6	23.4	16.6
Beam steering LDs-VLC	5.37	4.54	5.37	4.54	5.37	4.54	5.37
Fully Adaptive LDs-VLC	36.7	38.5	36.7	38.5	36.7	38.5	36.7

It should be noted that the channel bandwidth is negatively affected by the number of light spots seen within the pixel's FOV, because when the number of spots increases this can result in the introduction of a time delay between the signals received from the spots within the receiver's FOV, and hence this limits the bandwidth. For instance, the impulse response of non-adaptive systems (systems that do not employ the delay adaption approach) has many peaks (see Fig. 11), which increases the delay spread for these systems (see Fig .12). However, when the delay adaptation technique is combined with those systems the channel bandwidth increases dramatically, as shown in Table II.

D. SNR

Due to the symmetry of the room, the results for x=3 equal the results for x=1, therefore only the x=1m and x=2m results are shown along the y-axis. In this paper, we consider a low data rate (30 Mbps) to enable a comparison with previous work [12]. A higher data rate of 20 Gbps is also considered. For a bit rate of 30 Mbps we employed the PIN-FET trans-impedance preamplifier used in [31]. For the higher data rate we used the PIN-HMET receiver designed in [43]. Fig. 13 illustrates the SNR_{SB} and SNR_{MRC} of the imaging LDs-VLC, DAT imaging LDs-VLC, beam steering LDs-VLC and fully adaptive LDs-VLC systems at low data rates (30Mbps). It is observed that the adaptive systems (systems that applied the delay adaptation technique) did not give any advantage over non-adaptive systems at low data rates due to the high channel bandwidth achieved by all systems, which guarantees low ISI at the low operating bit rate considered (30 Mbps). The beam steering LDs-VLC and fully adaptive LDs-VLC systems achieved about a 10 dB SNR gain over the imaging LDs-VLC and DAT imaging LDs-VLC systems when the beam steering technique is applied with the low data rate systems. In addition, it can be seen that the difference between SB and MRC is about 4 dB on average in all systems. This is because the MRC receiver effectively produces an SNR

which is equal to the sum of the SNRs experienced by all the pixels versus SB which simply chooses the pixel with the best SNR. Moreover, the number of RGB-LDs visible within the pixel's FOV is a key to achieving a high SNR. As a result of this fact, the beam steering technique has the ability to enhance the SNR by directing a part of the white light towards the receiver location and thus increases the number of LOS components within the pixel's FOV. To evaluate the performance of our four systems at higher bit rates, the SNR is calculated at 20 Gbps.
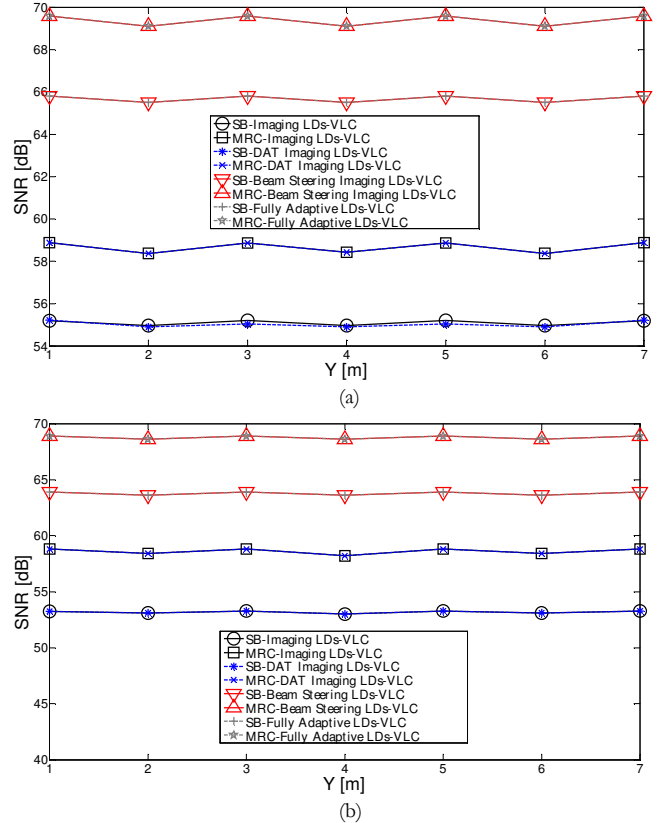

(a)

(b)

Fig. 13: SNR of four systems (imaging LDs-VLC, DAT imaging LDs-VLC, beam steering LDs-VLC and fully adaptive LDs-VLC) when operated at 30 Mbps and using two combing schemes (SB and MRC), (a) at x=1m and (b) at x=2m along the y-axis.

Fig. 14 shows the SNR_{SB} and SNR_{MRC} of the four VLC systems at 20 Gbps. To achieve a BER of 10^{-9} in OOK, a SNR of 15.6 dB is required [32], [53]. It can be noted that the fully adaptive system has the ability to provide SNR values higher than this required value in all the receiver locations. The fully adaptive VLC system outperforms other systems in terms of SNR, it achieves about a 15 dB SNR gain over the DAT imaging LDs-VLC system in the middle of the room. This significant improvement in the SNR level is attributed to the ability of the beam steering technique to steer a part of the light towards the receiver location and thus increase the power received by the pixels. Although, the beam steering technique increases the power level at the receiver with the beam steering LDs-VLC system as shown in Fig. 11 and increases the SNR at low data rates as shown in Fig. 13, at high data rates (20 Gbps) the performance decreases dramatically. This is due to the high multipath dispersion and ISI at the high data rates. Therefore, when the delay adaptation technique is combined with the beam steering system (fully adaptive system) we can achieve considerable enhancements in terms of SNR and 3 dB channel bandwidth, as shown in Table II and Fig. 14. In addition, the delay adaptation technique adds a degree of freedom to the link design for the adaptive systems (DAT imaging and fully adaptive VLC), resulting in VLC systems that

11

can provide higher SNR compared to the non-adaptive systems (imaging LDs-VLC and beam steering LDs-VLC). At x=1m, the SNR fluctuations in the non-adaptive systems due to ISI and multipath propagation can be mitigated by employing the delay adaptation approach. Moreover, when the VLC receiver moves along x=1m in all four systems, we noticed that it has a high SNR compared to when the receiver moves along x=2m, and this is due to the high multipath, ISI and path loss in the middle of the room (x=2m).
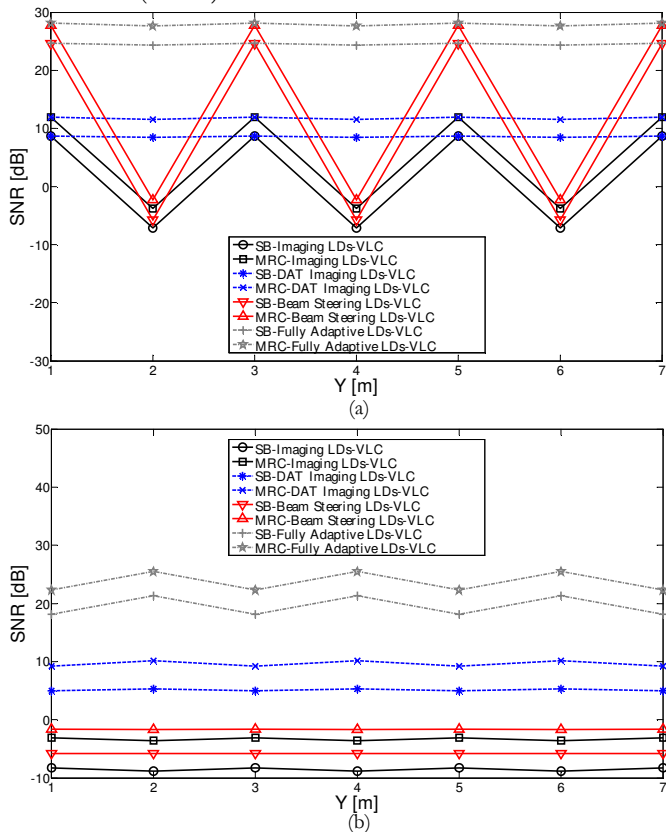

Fig. 14: SNR of four systems (imaging LDs-VLC, DAT imaging LDs-VLC, beam steering LDs-VLC and fully adaptive LDs-VLC) when operated at 20 Gbps and using two combing schemes (SB and MRC), (a) at x=1m and (b) at x=2m along the y-axis.

Table III presents the BER values corresponding to the achieved SNRs at 20 Gbps for the imaging LDs-VLC, DAT imaging LDs-VLC, beam steering LDs-VLC and fully adaptive LDs-VLC systems respectively at line x=2m when using SB (due to room symmetry, we calculated BER for 1 m to 4 m along the y axis). It can clearly be seen that the fully adaptive LDs-VLC system has the best performance compared to the other systems. The highest value of BER in the fully adaptive LDs-VLC system is equal to 4.1×10^{-16}, and this value can provide a strong communication link.

TABLE III
BER PERFORMANCE OF THE PROPOSED SYSTEMS AT x=2m

System	BER			
	Receiver Locations along the y-axis, y [m]			
	1	2	3	4
Imaging LDs-VLC	7.9×10^{-1}	9.9×10^{-1}	7.9×10^{-1}	9.9×10^{-1}
DAT Imaging LDs-VLC	4.7×10^{-2}	3.9×10^{-2}	4.7×10^{-2}	3.9×10^{-2}
Beam steering LDs-VLC	6.8×10^{-1}	6.8×10^{-1}	6.8×10^{-1}	6.8×10^{-1}
Fully Adaptive LDs-VLC	4.1×10^{-16}	9.3×10^{-32}	4.1×10^{-16}	9.3×10^{-32}

VIII. ROBUSTNESS TO SHADOWING, SIGNAL BLOCKAGE AND MOBILITY

Shadowing, signal blockage and mobility are among the main impairments that impact the performance of VLC systems in indoor environments. Therefore, we extended the analysis and evaluation of the performance of the proposed systems to a harsh indoor environment with mobility. The simulation was conducted in a room that was comparable in dimensions to that considered in Section II (see Fig. 1). Fig. 15 illustrates a realistic room environment where a door, windows, cubicle partitions, bookshelves and furniture are all present. The ceiling and the walls that surround the windows have a diffuse reflectivity of 0.8. The door and three glass windows are considered to not reflect any signal, therefore their diffuse reflectivities are set to zero. Two of the walls: x=4m (excluding the door) and y=8m were covered by filling cabinets and bookshelves with a diffuse reflectivity of 0.4. It was assumed that signals that encountered a physical barrier were either blocked or absorbed. Additionally, desks, tables and chairs inside the realistic room have similar reflectivities to the floor (i.e. 0.3). The complexity of the environment in this room results in shadowing created by low reflectivity objects and physical partitions. Comparisons were performed between the fully adaptive and DAT imaging LDs-VLC systems in two different environments (i.e. room A that is an empty room (see Fig. 1) and room B that is a realistic room (see Fig. 15)) when operating at 20 Gbps with full mobility. The complex environment in this room results in shadowing created by low reflectivity objects and physical partitions. In this section, the results of the adaptive systems are compared in rooms A and B in terms of impulse response, path loss and SNR. We have considered a mobile user with a speed of 1 m/s moving along the y-axis in the lines x=1m, x=2m and x=3m, the results in this Section are presented in two places in room 1) when the user is inside a mini cubicle (x=1m and x=3m along the y-axis) and 2) when the mobile user is in the middle of the room (x=2m and along the y-axis). In this Section a simulation package based on a ray-tracing algorithm was developed using MATLAB to compute the impulse response of the proposed systems. Additional features were introduced for a realistic room.
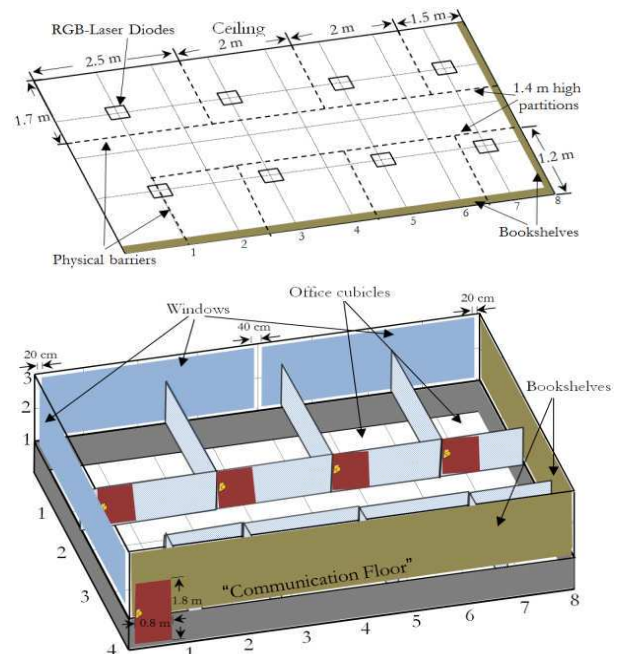

Fig. 15: Realistic room with a number of rectangular-shaped cubicles with surfaces parallel to the room walls, a door, three large glass windows and furniture, such as bookshelves and chairs.

12

In the realistic environment for each receiver location the first step is to check the availability of LOS components (certain conditions were introduced to the simulator to check the existence of LOS, 1st and 2nd order reflection components in each location) then the received power due to 1st and 2nd order reflections is also calculated.

A. Impulse responses

It is observed that in all room locations both systems have the ability to establish LOS links between the transmitters and receiver, which is due to a good distribution of RGB-LDs on the ceiling. For example, Fig. 16 shows the impulse responses at the room centre (2 m, 4 m, 1 m) for the fully adaptive system and for the DAT imaging LDs-VLC system in rooms A and B (room A is an empty room and room B is a realistic environment). In both room scenarios for the two systems the LOS components are the same. However, the power collected from the signals coming to the receiver from the ceiling, strip walls that surround the windows and bookshelves is decreased due to many reasons. Firstly, the physical partitions prevent rays from reaching the receiver. In addition, the reflectivity of the two windows is zero, which means no signals will be received from the two walls at $x=0$ and $y=0$. Moreover, the bookshelves have a reflectivity of 0.4, and this reduces the power of the signals received from them. However, we should note that the LOS link has the largest amount of received power and the reduction in received power from reflections is negligible. For instance, the associated power at the room centre position for the fully adaptive system in room A is 47.46 μW whereas it was 47.41 μW in room B.
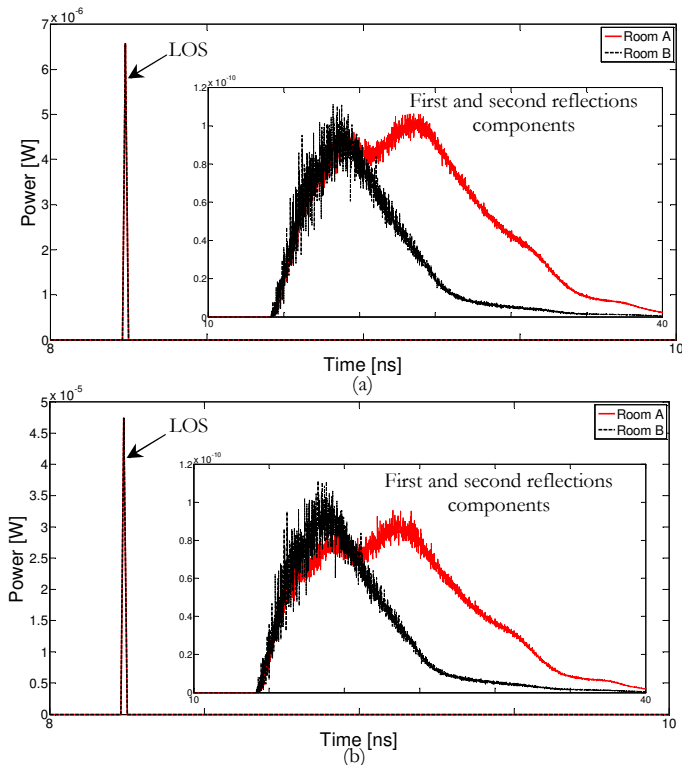

Fig. 16: Impulse responses of the two systems (a) DAT imaging LDs-VLC and (b) fully adaptive LDs-VLC in two different environments at room centre.

B. Path loss analysis

One of the main targets of any communication system is to achieve high SNR at the receiver. The SNR in OW systems is based on the square of the received optical signal power, receiver

and ambient noises [37]. Therefore, the average received optical power and path loss explains part of the main VLC system performance in the two different environments. Optical path loss can be defined as [54]:

$$PL(dB) = -10log_{10}(\int h(t)dt) \qquad (14)$$

where $h(t)$ is the system impulse response. Fig. 17 illustrates the path loss distributions for rooms A and B at $x=1$m, $x=2$m and $x=3$m along the y-axis. It can be seen that the path loss for the two systems is comparable in both room scenarios. The path loss increased less than 0.5 dB when both systems were evaluated in room B. This insignificant increase in the path loss is attributed to the fact that our systems have the ability to establish LOS links in both rooms (i.e. A and B), which leads to similar performances when operated in different environments. Therefore both systems possess robustness against shadowing and mobility and they are able to achieve similar performance levels in an empty room and a realistic environment.
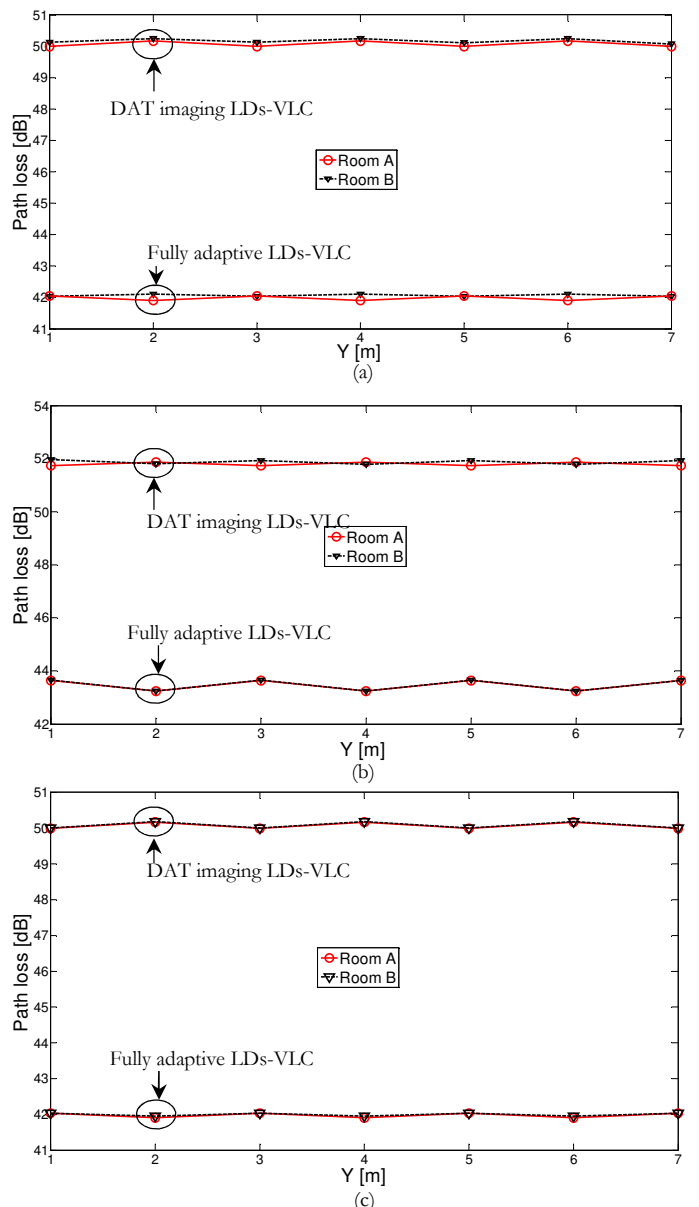

Fig. 17: Path loss of the DAT imaging LDs-VLC and fully adaptive LDs-VLC systems in two different environments (a) at $x=1$m, (b) at $x=2$m and (c) at $x=3$m along the y-axis.

13

It can be noted that the path loss in the two systems at x=3m is better than (slightly lower) that at x=1m in the realistic environment. This is due to the presence of windows which is close to side x=1m of the room and the presence of bookshelves at the other side (x=4m). In DAT imaging LDs-VLC system when the receiver position was close to the windows (along x=1m), for example, at point (x=1m and y=1m) the path loss becomes higher because the received power from the reflections is very low (glass windows are considered to not reflect any signal). However, when the receiver moves towards the other side of the room (i.e., receiver positions close to bookshelves), for instance, at point x=3m and y=1m) the path loss decreases due to the power received from the signals reflected by the bookshelves. In addition, it can be seen that the path loss in the two systems is higher when the receiver moves along x=2m. This is due to the larger distance between the receiver and transmitter.

C. SNR analysis

Fig. 18 shows the SNR of four systems (imaging LDs-VLC, DAT imaging LDs-VLC, beam steering LDs-VLC and fully adaptive system) at x=1m, x=2m and x=3m along the y-axis over the communication floor for different environments (i.e. rooms A and B). In rooms A and B both adaptive systems have comparable results, there was very low degradation in the SNR when both systems operated in room B. This is attributed to the ability of our adaptive systems to adapt to such an environment. Also, it should be noted that the results in Fig. 18 are in agreement with the general observation made in Fig. 17. For example, for the DAT imaging LDs-VLC system at the point x=1m and y=4m, the path loss is highest resulting in the lowest SNR. Similar behaviour was observed when comparing Fig. 17 and Fig. 18 for the fully adaptive system.
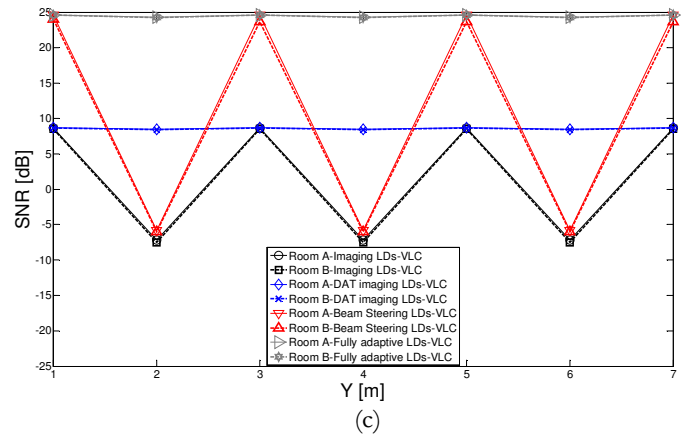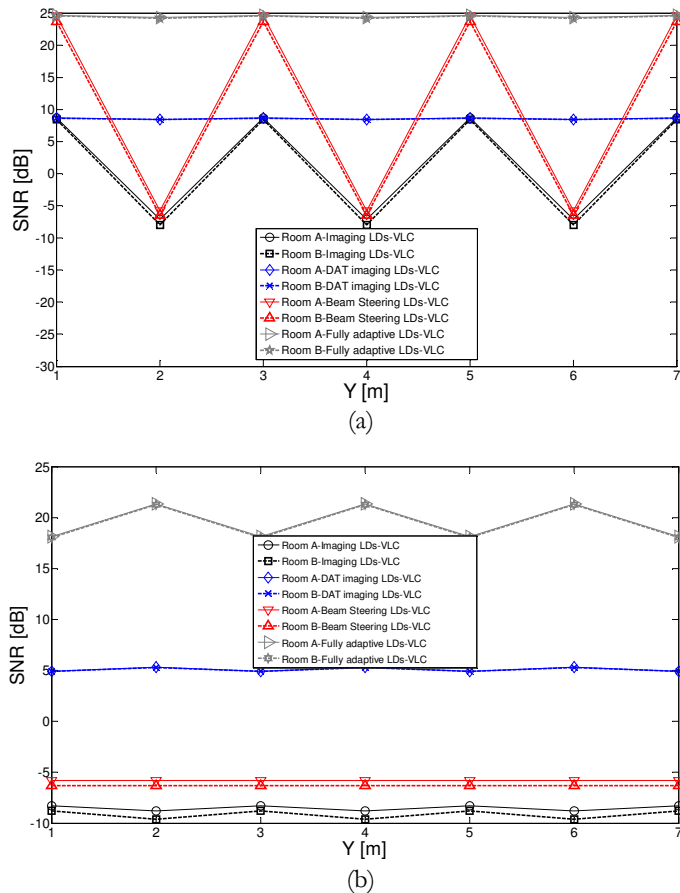

Fig. 18: SNR_{SB} of four systems (imaging LDs-VLC, DAT imaging LDs-VLC, beam steering LDs-VLC and fully adaptive LDs-VLC) when operated at 20 Gbps in two different room scenarios at (a) x=1m, (b) at x=2m and (c) at x=3m along the y-axis.

In a realistic environment when the user is inside a mini cubicle (x=1m and x=3m and along the y-axis) the SNRs of the proposed systems are comparable. However, it can be noted that the SNR at x=1m is lower than at x=3m. This is due to reflections from windows (walls close to x=1m is converted to windows in realistic room) which are set to zero (transparent windows), while the other two walls (walls close to x=3m) in room B are covered by filling cabinets and bookshelves. This means that the power contribution from the reflections at x=1m is minimal and this reduced the SNR. In addition, it should be noted that the systems that employ the delay adaptation technique (DAT imaging and fully adaptive VLC) can provide higher SNR compared to the non-adaptive systems (imaging LDs-VLC and beam steering LDs-VLC).

To achieve optimum results in the fully adaptive system the SNR values of D&C algorithm used in LEA should be monotonic. It can be noted that the fully adaptive system has smooth SNR at all relevant locations in the room (see Figs. 14 and 18).

Table IV shows the BER at 20 Gbps of the proposed systems (imaging LDs-VLC, DAT imaging LDs-VLC, beam steering LDs-VLC and fully adaptive LDs-VLC) at line x=2m when using SB. It can be noted that the fully adaptive LDs-VLC system has the best performance compared to the other systems. In the realistic environment, the BER of the fully adaptive VLC system has increased slightly compared to an empty room. However, this increase does not severely affect the performance of the system; for example, the maximum value of BER provided by the fully adaptive LDs-VLC system is equal to 6.9×10^{-16}.

TABLE IV
BER PERFORMANCE OF THE PROPOSED SYSTEMS AT x=2m

System	BER			
	Receiver Locations along the y-axis, y [m]			
	1	2	3	4
Imaging LDs-VLC	9.8×10^{-1}	9.9×10^{-1}	9.8×10^{-1}	9.9×10^{-1}
DAT Imaging LDs-VLC	4.8×10^{-2}	4×10^{-2}	4.8×10^{-2}	4×10^{-2}
Beam steering LDs-VLC	7×10^{-1}	7×10^{-1}	7×10^{-1}	7×10^{-1}
Fully Adaptive LDs-VLC	6.9×10^{-16}	3.8×10^{-31}	6.9×10^{-16}	3.8×10^{-31}

IX. High Speed Adaptive Mobile VLC System

The high channel bandwidth achieved through the delay adaptation technique coupled with the additional SNR accomplished by the beam steering technique, can be used to provide high data rates (20 Gbps and beyond) with the new VLC system. The PIN-HMET optical receiver proposed by Gimlett [43] was used for the fully adaptive VLC system to operate at 20 Gbps. The noise current spectral density for this preamplifier is $12 \text{ pA}/\sqrt{\text{Hz}}$ and the preamplifier has a bandwidth of 16 GHz. Through the use of a suitable filter the preamplifier bandwidth can be limited to 14 GHz. The optimum receiver bandwidth is 0.7 times the bit rate according to Personick's analysis [55]. Transmitters for data rates of up to 40 Gbps are established in fibre systems [56], therefore the rise and fall times of the LDs based transmitter is not considered in this paper. The OOK modulation format is used with intensity modulation and direct detection. The OOK modulation is an appropriate modulation scheme for high data rates in OW systems [57] due to its simplicity, however higher order modulation formats can be investigated. Adaptive equalisation can be used to further reduce the ISI [58]. The SNR calculations in equation (5) take into account eye closure ($P_{s1} - P_{s0}$), and therefore the SNR values reported consider ISI and receiver preamplifier noise. The imaging LDs-VLC, DAT imaging LDs-VLC and beam steering LDs-VLC systems performed identically at a bit rate of 30 Mbps, and this is evident due to the excess channel bandwidth available. ISI increased noticeably at 20 Gbps which results in significant SNR degradations. The fully adaptive LDs-VLC system can offers high SNR (18 dB at the least successful point) and bandwidth of more than 36 GHz (see Table II), which enables it to support data rates of 20 Gbps. Fig. 14 shows that an SNR gain of 27 dB can be achieved when the fully adaptive system is used instead of the beam steering system in the middle of the room (worst case scenario). This improvement is due to the use of the delay adaptation technique with beam steering (fully adaptive system), and it significantly reduces the effect of ISI and multipath dispersion. The SNR results of the fully adaptive system in the real environment (see Fig. 18) show that our proposed system achieves an SNR_{SB} of 18 dB under the worst case scenario (at point x=2, y=1, 3, 5 and 7 in Fig. 18b), which is greater than the 15.6 dB needed to achieve 10^{-9} BER. This SNR is obtained when multipath propagation, shadowing, signal blockage and mobility are all present. The feedback link is vital for the proposed systems as it affects directly the performance of the systems. The feedback channel is used to send information (such as SNR measured for STB algorithm and mean delay for DAT algorithm) at very low data rate. If any error occurs in this channel, this will degrade the performance of the fully adaptive system. The feedback channel operates at a very low data rate, which means that SNRs in excess of 33 dB can be achieved at data rates up to 30 Mbps [32], [44]. This in turn means that the BER achieved in the feedback channel is extremely small which would be considered an almost ideal communication link. However, Forward error correction coding (FEC) can be used to ensure that any errors in the feedback channel are minimized.

Simulation results have shown that LEA and beam steering coupled with imaging receiver detection, can significantly improve performance in the proposed system (beam steering LDs-VLC system). However this is at the cost of complexity in the design of beam steering LDs-VLC. The complexity is associated with the computation time required to identify the optimum location to perform beam steering. For example, in a typical room with dimensions of $4m \times 8m \times 3m$ (width ×

length × height), LEA generates a single spot which scans the communication floor changing the beam angle associated with the spot between $-70^°$ and $70^°$ in steps of $0.28^°$, a total of 224 possible locations, which requires 224 ms adaptation time in order to identify the optimum location. The time required to generate the hologram with optimum spot angles and powers can therefore be estimated. If the fully adaptive VLC system uses the output plane phase optimization (OPPO) algorithm proposed in [59], then the total computation is [59]:

$$t_{oppo} = 5 \times p \times S^2 + S \times M \times N, \tag{15}$$

where $M \times N$ is the number of hologram pixels, S is the number of spots on the output plane (ceiling), p is the phase level. The first term ($5 \times p \times S^2$, complex operations) represent the computations needed for designing the temporary hologram using direct binary search (DBS) and the second term ($S \times M \times N$, complex operations) represents the computation of the hologram using discrete Fourier transform (DFT). If $M = N = 200$, S=1 and p=8, then:

$$t_{oppo} = 40 + 40000. \tag{16}$$

The computation for designing the temporary hologram can be ignored based on the study in [59]. If each operation in the optimization of the hologram is carried out in 1 µs then the total time required to generate a hologram is 40 ms. Therefore, the fully adaptive system can achieve 100% of the specified data rate when it is stationary, and 88.8% (40 ms (generate hologram) + 72 ms (DAT)) in the case of user movement, i.e., 20 Gbps when it is stationary and about 17.76 Gbps when there are environmental changes (user or object movement in the room).

The PHY layer of the IEEE 802.15.7 standard for VLC system supports three different types of modulation schemes; OOK, pulse position modulation (PPM) and colour shift keying (CSK) [A]. In this work all the proposed systems employ an OOK modulation scheme that adds simplicity to the VLC system. Using PPM or CSK imposes more system complexity compared to OOK.

X. Conclusions

In this paper, for the first time to best of our knowledge, we introduced beam steering and location estimation algorithms for a mobile multi-gigabit VLC system. We also combined these algorithms with the concept of delay adaptation to produce a fully adaptive VLC system that has the ability to achieve 20 Gbps with full receiver mobility in a realistic indoor environment. The location estimation algorithm (LEA) estimates the best locations to steer the beam to by scanning a single beam over the communication floor and computing the resultant SNR for every single beam. We later introduced a fast version based on a divide and conquer algorithm.

We investigated the effect of beam steering on the illumination and found that up to 20% of the light from the RGB-LDs can be beam steered towards the receiver position to improve SNR without affecting the illumination. The beam steering technique steers 20% of the white light from a certain RGB-LDs light unit (close to receiver) towards the optimum location that was found by LEA to maximise the SNR. In addition, at a low data rate (30 Mbps) our fully adaptive system offers an SNR improvement of 10 dB over the imaging LDs-VLC system when using the MRC approach. At a high data rate (20 Gbps) a 29 dB SNR gain is

achieved when the fully adaptive system replaces the imaging LDs-VLC system under the worst case scenario, and these improvements in the SNR enable our fully adaptive system to provide a BER of better than 10^{-9} at all receiver locations when operated at 20 Gbps in a harsh room environment.

We evaluated the performance of the fully adaptive system in a harsh environment with full mobility. The results show that our proposed system has the ability to maintain a LOS link at any location in the room and this gives immunity against shadowing and mobility.

Furthermore, the delay adaptation technique was combined with the beam steering technique and location estimation algorithm to mitigate the effect of ISI and multipath dispersion. The delay adaptation adjusts the switching times of the signals in a fashion that allows the signals to reach the receiver at the same time. The significant improvements in channel bandwidth and SNR enhance the performance of our VLC system and enable it to operate at higher data rates (20 Gbps and beyond). Moreover, the beam steering LDs-VLC system can achieve 100% of the data rate (20 Gbps) when it is stationary and 70.4% (14 Gbps) in the case of user movement, and this is due to the time needed (296 ms) for the adaptation process. Also, we have introduced new finite vocabulary holograms for VLC where the holograms are pre-calculated and stored in our proposed system, thus the time required to find optimum location to perform beam steering technique reduced from 224 ms to 40 ms.

To the best of our knowledge, the data rates achieved by our proposed system (i.e. 20 Gbps for a stationary user and 14 Gbps for a mobile user) are the highest data rates to date for an indoor VLC system with simple modulation format (OOK) and without the use of relatively complex wavelength division multiplexing approaches.

Future work will address methods to accelerate the location estimation algorithm and make the time required to find the receiver location less than 224 ms.

REFERENCES

[1] D. C. O Brien, L. Zeng, H. L. Minh, G. Faulkner, J. W. Walewski, and S. Randel, "*Visible light communications: Challenges and possibilities,*" 19th International Symposium on Indoor and Mobile Radio Communications, (PIMRC), pp.1-5, 2008.

[2] A. T. Hussein, and J. M. H. Elmirghani, "*A Survey of Optical and Terahertz (THz) Wireless Communication Systems,*" IEEE Communications Surveys & Tutorials, (to be submitted), 2015.

[3] P. A. Haigh, T. T. Son, E. Bentley, Z. Ghassemlooy, H. Le Minh and L. Chao, "*Development of a Visible Light Communications System for Optical Wireless Local Area Networks,*" in Proc. IEEE Computing Communications and Applications Conference (ComComAp), pp.315-355, 2012.

[4] K. K. Wong, and T. O'Farrell, "*Spread spectrum techniques for indoor wireless IR communications,*" IEEE Wireless Communications, vol.10, no.2, pp.54-63, 2003.

[5] D. Tsonev, H. Chun, S. Rajbhandari, J. McKendry, S. Videv, E. Gu, M. Haji, S. Watson, A. Kelly, G. Faulkner, M. Dawson, H. Haas, and D. O'Brien, "*A 3-Gb/s Single-LED OFDM-Based Wireless VLC Link Using a Gallium Nitride μLED,*" IEEE Photonics Technology Letter, vol.26, no.7, pp.637–640, 2014.

[6] S. Dimitrov, and H. Haas, "*Principles of LED Light Communications: Towards Networked Li-Fi,*" Cambridge University Press, 2015.

[7] T. Fath, and H. Haas, "*Performance comparison of MIMO techniques for optical wireless communications in indoor environments,*" IEEE Transactions on Communications, vol.61, no.2, pp.733-742, 2013.

[8] G. Cossu, A. M. Khalid, P. Choudhury, R. Corsini, and E. Ciaramella, "*3.4 Gbit/s visible optical wireless transmission based on RGB LED,*" Optics express, vol.20, no.26, pp.501-506, 2012.

[9] A. Neumann, J. J. Wierer, W. Davis, Y. Ohno, S. Brueck, and J. Y. Tsao. "*Four-color laser white illuminant demonstrating high color-rendering quality,*" Optics express, vol.19, no.104, pp.982-990, 2011.

[10] K. A. Denault, M. Cantore, S. Nakamura, S. P. DenBaars, and R. Seshadri, "*Efficient and stable laser-driven white lighting,*" AIP Advances, vol.3, no.7, pp.1-6 2013.

[11] D. S. Weber, A. Buck, and D. Christian Amann, "*Laser Light in the BMW i8 Design, System Integration and Test,*" ATZ worldwide, vol.116, no.9, pp.44-49, 2014.

[12] A. T. Hussein, and J.M.H. Elmirghani, "*Mobile Multi-gigabit Visible Light Communication System Employing Laser Diodes, Imaging Receivers and Delay Adaptation Technique in Realistic Indoor Environment,*" Journal of Lightwave Technology, vol.33, no.15, 2015.

[13] A. T. Hussein, and J.M.H. Elmirghani, "*High-Speed Indoor Visible Light Communication System Employing Laser Diodes and Angle Diversity Receivers,*" 17th International Conference in Transparent Optical Networks (ICTON), 2015.

[14] A. T. Hussein, and J.M.H. Elmirghani, "*Performance Evaluation of Multi-gigabit Indoor Visible Light Communication System,*" The 20th European Conference on Network and Optical Communications, (NOC), 2015.

[15] A. T. Hussein, and J.M.H. Elmirghani, "*10 Gbps Mobile Visible Light Communication System Employing Angle Diversity, Imaging Receivers and Relay Nodes,*" Journal of Optical Communications and Networking, vol.7, issue 8, 2015.

[16] D. Tsonev, S. Videv, and H. Haas, "*Towards a 100 Gb/s visible light wireless access network,*" Optics express, vol. 23, issue 2, pp.1627–1637, 2015.

[17] C. Lee, C. Zhang, M. Cantore, R. M. Farrell, S. H. Oh, T. Margalith, J. S. Speck, S. Nakamura, J. E. Bowers, and S. P. DenBaars, "*4 Gbps direct modulation of 450 nm GaN laser for high-speed visible light communication,*" Optics express, vol.23, no.12, pp.6232-16237, 2015.

[18] M. T. Alresheedi, and J.M.H. Elmirghani, "*Performance evaluation of 5 Gbit/s and 10 Gbit/s mobile optical wireless systems employing beam angle and power adaptation with diversity receivers,*" IEEE Journal on Selected Areas in Communications, vol.29, no.6, pp.1328-1340, 2011.

[19] F. E. Alsaadi, and J. M. H. Elmirghani, "*High-speed spot diffusing mobile optical wireless system employing beam angle and power adaptation and imaging receivers,*" Journal of Lightwave Technology, vol.28, no.16, pp.2191–2206, 2010.

[20] D. P. Resler, D. S. Hobbs, R. C. Sharp, L. J. Friedman, and T. A. Dorschner, "*High-efficiency liquid-crystal optical phased-array beam steering,*" Optics letters vol.21, no.9, pp. 689-691, 1996.

[21] L. Wu, Z. Zhang and H. Liu, "*Transmit Beamforming for MIMO Optical Wireless Communication Systems,*" Wireless Personal Communications, vol.78, issue 1, pp 615-628, 2014.

[22] S. Kim, and S. Kim, "*Wireless optical energy transmission using optical beamforming,*" Optical Engineering, vol.2, no.4, pp.205-210, 2013.

[23] VISIBLE LIGHT COMMUNICATION SYSTEM: NAKAGAWA GROUP, 2010; AVAILABLE FROM: http://www.youtube.com/watch?v=QEh5f49LsB4. Last access date 15 July 2015.

[24] K. Panta, and J. Armstrong, "*Indoor localisation using white LEDs,*" Electronics letters, vol.48, no.4, pp.228-230, 2012.

[25] S. Jung, S. Hann, and C. Park, "*TDOA-based optical wireless indoor localization using LED ceiling lamps,*" IEEE Transactions on Consumer Electronics, vol.57, no.4, pp.1592-1597, 2011.

[26] W. Zhang, and M. Kavehrad, "*Comparison of VLC-based indoor positioning techniques,*" Broadband Access Communication Technologies, vol.86, no.45, pp.226-232, 2013.

[27] M. T. Alresheedi, and J.M.H. Elmirghani, "*High-Speed Indoor Optical Wireless Links Employing Fast Angle and Power Adaptive Computer-Generated Holograms with Imaging Receivers,*" IEEE Journal on Communications, accepted, 2015.

[28] M. T. Alresheedi, and J.M.H. Elmirghan, "*Hologram Selection in Realistic Indoor Optical Wireless Systems with Angle Diversity Receivers,*" IEEE Journal of Optical Communications and Networking, vol.7, no.8, pp.797-813, 2015.

[29] F. E. Alsaadi, M. A. Alhartomi, and J. M. H. Elmirghani, "*Fast and efficient adaptation algorithms for multi-gigabit wireless infrared systems,*" Journal of Lightwave Technology, vol. 31, no. 23, pp. 3735–3751, 2013.

[30] F. E. Alsaadi, and J.M.H. Elmirghani, "*Adaptive mobile line strip multibeam MC-CDMA optical wireless system employing imaging detection in a real indoor environment,*" IEEE Journal on Selected Areas in Communications, vol.27, no.9, pp.1663-1675, 2009.

[31] P. Djahani, and J. M. Kahn, "*Analysis of Infrared Wireless Links Employing Multibeam Transmitter and Imaging Diversity Receivers,*" IEEE Transactions on Communication, vol.48, no.12, pp.2077-2088, 2000.

[32] M. T. Alresheedi, and J.M.H. Elmirghani, "*10 Gb/s Indoor Optical Wireless Systems Employing Beam Delay, Power, and Angle Adaptation Methods With Imaging Detection,*" Journal of Lightwave Technology, vol.30, no.12, pp.1843-1856, 2012.

[33] F. R. Gfeller, and U. H. Bapst, "*Wireless in-house data communication via diffuse infrared radiation*," Proc. IEEE, vol.67, no.11, pp.1474-1486, 1979.

[34] T. Komine, and M. Nakagawa, "*Fundamental analysis for visible-light communication system using LED lights*," IEEE Transactions on Consumer Electronics, vol.50, no.1, pp.100-107, 2004.

[35] J. R. Barry, J. M. Kahn, W. J. Krause, E. A. Lee, and D. G. Messerschmitt, "*Simulation of multipath impulse response for indoor wireless optical channels*," IEEE Journal on Selected Areas in Communications, vol.11, no.22, pp.367-379, 1993.

[36] "*European standard EN 12464-1: Lighting of indoor work places*", [online] Available:*http://www.etaplighting.com/uploadedFiles/Downloadable_documentation/documentatie/EN12464_E_OK.pdf*. Last access date 15 July 2015.

[37] J. M. Kahn, and J.R. Barry, "*Wireless infrared communications*," Proceedings of the IEEE, vol.85, no.2, pp.265-298, 1997.

[38] A. G. Al-Ghamdi, and J.M.H. Elmirghani, "*Analysis of diffuse optical wireless channels employing spot-diffusing techniques, diversity receivers, and combining schemes*," IEEE Transactions on Communications, vol.52, no.10, pp.1622-1631, 2004.

[39] M. Biagi, T. Borogovac, and T.D.C. Little, "*Adaptive Receiver for Indoor Visible Light Communications*," Journal of Lightwave Technology, vol.31, no.23, pp. 3676-3686, 2013.

[40] A. G. Al-Ghamdi, and J. M. H. Elmirghani, "*Line strip spot-diffusing transmitter configuration for optical wireless systems influenced by background noise and multipath dispersion*," IEEE Transactions on Communication, vol.52, no.1, pp.37-45, 2004.

[41] M. A. Alhartomi, F.E. Alsaadi, and J.M.H. Elmirghani, "*Mobile optical wireless system using fast beam Angle, delay and power adaptation with angle diversity receivers*," 14th International Conference in Transparent Optical Networks (ICTON), 2012.

[42] J. M. Senior, and M. Yousif Jamro, "*Optical fiber communications: principles and practice*," 3rd edition Pearson Education, 2009.

[43] J. A. Gimlett, "*new low noise 16 GHz PIN/HEMT optical receiver*," 14th European Conference on in Optical Communication, (ECOC 88), vol.1, no.292, pp.13-16, 1988.

[44] F. E. Alsaadi, and J. M. H. Elmirghani, "*Beam power and angle adaptation in multibeam 2.5 gbit/s spot diffusing mobile optical wireless system*," IEEE journal on selected areas in communications, vol.28, issue 6, pp.913 - 927, 2010.

[45] *IEEE Standard for Local and Metropolitan Area Networks-Part 15.7: Short-Range Wireless Optical Communication Using Visible Light*, pp.1-309, 2011.

[46] M. Biagi, S. Pergoloni, and A. M. Vegni, "*LAST: a Framework to Localize, Access, Schedule and Transmit in Indoor VLC Systems*," IEEE Journal of Lightwave Technology, vol.33, no.9, pp.1872-1887, 2015.

[47] J. Davis, D. E. McNamara, D. M. Cottrell, and Tomio Sonehara, "*Two-dimensional polarization encoding with a phase-only liquid-crystal spatial light modulator*," Applied Optics vol.39, no.10, pp.1549-1554, 2000.

[48] "*Spatial Light Modulators*", [online], Available: http://holoeye.com/wp-content/uploads/Spatial_Light_Modulators.pdf. Last access date 15 July 2015.

[49] M. Tolstrup, "*Indoor Radio Planning: A Practical Guide for Gsm, Dcs, Umts, Hspa and Lte*," John Wiley & Sons., 2011.

[50] P. Viswanath, D. N. C. Tse, and R. Laroia, "*Opportunistic beamforming using dumb antennas*," IEEE Transactions on Information Theory, vol.48, no.6 pp.1277-1294, 2002.

[51] P. Carnevali, L. Coletti, and S. Patarnello, "*Image processing by simulated annealing*," IBM J. Res. Develop., vol. 29, no. 6, pp. 569–579, 1985.

[52] M. A. Seldowitz, J. P. Allebach, and D. E. Sweeney, "*Synthesis of digital holograms by direct binary search*," Appl. Opt., vol. 26, pp. 2788– 2798, 1987.

[53] A. P. Tang, J.M. Kahn, and H. Keang-Po, "*Wireless infrared communication links using multi-beam transmitters and imaging receivers*," IEEE International Conference on Communications (ICC), Converging Technologies for Tomorrow's Applications, pp.180-186, 1996.

[54] A. G. Al-Ghamdi, and J.M.H. Elmirghani, "*Performance comparison of LSMS and conventional diffuse and hybrid optical wireless techniques in a real indoor environment*," IEE Proceedings Optoelectronics, vol.152, issue 4, pp.230-238, 2005.

[55] S. D. Personick, "*Receiver design for digital fiber optical communication system, Part I and II*," Bell System Technology Journal, vol.52, no.6, pp 843-886, 1973.

[56] "*40 GB/s optical transponder*," [Online]. Available: http://onelink.finisar.com/sites/default/files/pdf/54TRAAV2GPL-40G-SFF-NRZ-Transponder-product-brief-RevA.pdf. Last access date 15 July 2015.

[57] G. W. Marsh, and J. M. Kahn, "*50-Mb/s diffuse infrared free-space link using on-off keying with decision-feedback equalization*," IEEE Photon Technology Letter, vol. 10, no.6, pp.1268-1270, 1994.

[58] T. Komine, J. H. Lee, S. Haruyama and M. Nakagawa, "*Adaptive equalization system for visible light wireless communication utilizing multiple white LED lighting equipment*," IEEE Transactions on Wireless Communications, vol.8, no.6, pp.2892-2900, 2009.

[59] A. Georgiou, T. D. Wilkinson, N. Collings, and W. A. Crossland, "*Algorithm for computing spot-generating holograms*," Journal of. Optics: A pure and applied optics, vol. 10, no. 1, 2008.

Ahmed Taha Hussein received a B.Sc. (First Class Hons.) in electronic and electrical engineering from the University of Mosul, Iraq, in 2006 and an M.Sc. degree (with distinction) in communication systems from the University of Mosul, Iraq, in 2011. He is a Higher Committee for Education Developments in Iraq (HCED) Scholar and is currently working toward a Ph.D. degree in the school of Electronic and Electrical Engineering, University of Leeds, Leeds, UK.

Prior to his Ph.D. study, he worked as a Communication Instructor in Electronic and Electrical Engineering Department in the College of Engineering, University of Mosul, Iraq from 2006 to 2009. He also worked as a lecturer in the Electronic and Electrical Engineering Department in the College of Engineering, University of Mosul, Iraq from 2011 to 2012. He is the author of a number of published papers. In particular, his novel work on indoor visible light communication (VLC) system appears in the IEEE Journal of Lightwave Technology (JLT) and IEEE Journal of Optical Communications Networking (JOCN). Moreover, he has authored papers published in the International Conference on Transparent Optical Networks (ICTON) 2015 and the 20th European Conference on Network and Optical Communications (NOC) 2015. His research interests include performance enhancement techniques for visible light communication systems, visible light communication system design and indoor visible light communication networking.

Mohammed Alresheedi received a B.Sc degree (with First Class Honor) in Electrical Engineering from King Saud University, Riyadh, Saudi Arabia, in 2006 and an MSc degree (with Distinction) in Communication Engineering from Leeds University, United Kingdom, in 2009. He received the Ph.D. degree in Electronic and Electrical Engineering from Leeds University, United Kingdom in 2014. He is currently an Assistant Professor in the Electrical Engineering Department, King Saud University. His research interests include adaptive techniques for OW, OW systems design, indoor OW networking and visible light communications.

Prof. Jaafar M. H. Elmirghani is the Director of the Institute of Integrated Information Systems within the School of Electronic and Electrical Engineering, University of Leeds, UK. He joined Leeds in 2007 and prior to that (2000–2007) as chair in optical communications at the University of Wales Swansea he founded, developed and directed the Institute of Advanced Telecommunications and the Technium Digital (TD), a technology incubator/spin-off hub. He has provided outstanding leadership in a number of large research projects at the IAT and TD. He received the Ph.D. in the synchronization of optical systems and optical receiver design from the University of Huddersfield UK in 1994 and the DSc in Communication Systems and Networks from University of Leeds, UK, in 2014. He has co-authored Photonic switching Technology: Systems and Networks, (Wiley) and has published over 400 papers. He has research interests in optical systems and networks. Prof. Elmirghani is Fellow of the IET, Fellow of the Institute of Physics and Senior Member of IEEE. He was Chairman of IEEE Comsoc Transmission Access and Optical Systems technical committee and was Chairman of IEEE Comsoc Signal Processing and Communications Electronics technical committee, and an editor of IEEE Communications Magazine. He was founding Chair of the Advanced Signal Processing for Communication Symposium which started at IEEE GLOBECOM'99 and has continued since at every ICC and GLOBECOM. Prof. Elmirghani was also founding Chair of the first IEEE ICC/GLOBECOM optical symposium at GLOBECOM'00, the Future Photonic Network Technologies, Architectures and Protocols Symposium. He chaired this Symposium, which continues to date under different names. He was the founding chair of the first Green Track at ICC/GLOBECOM at GLOBECOM 2011, and is Chair of the IEEE Green ICT committee within the IEEE Technical Activities Board (TAB) Future Directions Committee (FDC), a pan IEEE Societies committee responsible for Green ICT activities across IEEE, 2012-present. He is and has been on the technical program committee of 34 IEEE ICC/GLOBECOM conferences between 1995 and 2015 including 15 times as Symposium Chair. He received the IEEE Communications Society Hal Sobol award, the IEEE Comsoc Chapter Achievement award for excellence in chapter activities (both in 2005), the University of Wales Swansea Outstanding Research Achievement Award, 2006, the IEEE Communications Society Signal Processing and Communication Electronics outstanding service award, 2009, a best paper award at IEEE ICC'2013, the IEEE Comsoc Transmission Access and Optical Systems outstanding Service award 2015 in recognition of "Leadership and Contributions to the Area of Green Communications" and received the GreenTouch 1000x award in 2015 for "pioneering research contributions to the field of energy efficiency in telecommunications". He is currently an editor of: IET Optoelectronics, Journal of Optical Communications, IEEE Communications Surveys and Tutorials and IEEE Journal on Selected Areas in Communications series on Green Communications and Networking. He is Co-Chair of the GreenTouch Wired, Core and Access Networks Working Group, an adviser to the Commonwealth Scholarship Commission, member of the Royal Society International Joint Projects Panel and member of the Engineering and Physical Sciences Research Council (EPSRC) College. He has been awarded in excess of £22 million in grants to date from EPSRC, the EU and industry and has held prestigious fellowships funded by the Royal Society and by BT. He is an IEEE Comsoc Distinguished Lecturer 2013-2016.